NTNU – Trondheim
Norwegian University of
Science and Technology

Numerical Modeling of Combined Hydraulics and Infiltration in Grassed Swales

Arve Grinden

Civil and Environmental Engineering
Submission date: June 2014
Supervisor: Sveinn T Thorolfsson, IVM

Norwegian University of Science and Technology
Department of Hydraulic and Environmental Engineering

Abstract

The aim of this thesis is to establish a numerical model capable of simulating combined infiltration and hydraulic discharge through grassed swales. The model is intended for making assessments of the hydraulics within urban drainage on a more detailed level than methods currently available.

An initial literature survey has been conducted, finding that research on the scientific field of hydraulics within sustainable urban drainage is scarce. The research available on drainage systems, such as grassed swales, is mainly focused on pollutant control through empirical research. An assessment is made that the need for detailed hydraulic investigations in order to fully understand swale runoff response is present, in order to fill this knowledge gap.

On this basis a numerical model implementing an explicit discretization St. Venant´s equation for dynamic overland flow, combined with Green Ampt´s infiltration equation for sloping surfaces has been established. This makes the model capable of handling varying flow conditions on a short time scale, as will be the case in urban runoff events. The model has been established in the MATLAB programming language and allows for a wide range of user input of hydraulic and infiltration parameters. Simulations have been conducted on constructed data in order to assess the effect of variations in input parameters and the model simulation range. The combined model yields results consistent with what is expected from the governing equations, given typical swale design parameters. Instabilities were encountered for high slopes combined with low Manning coefficients, and for infiltration media consisting of fine grained soil types. Some simplifications needed to be made in order to combine the infiltration and hydraulic flow, amongst the most important the introduction of an artificial threshold depth. This is due to the models inability to run as the flow depth approaches zero, and a stable threshold depth is set to $0.005\,m$. The main reason behind this is a severe limitation in computational time step range, where the hydraulic equations require very small time steps and the infiltration equation requires large time steps. Given a suitable time step, the model produces consistently satisfactory simulation results.

The model is expected to concur well with observed swale flow, given the needed calibration and verification. At the time of this thesis, suitable field data were not available such that model calibrations could not be conducted. If detailed modeling of depth approaching zero is needed, it should be considered implementing an implicit discretization in the hydraulic step.

Sammendrag

Målet med denne masteroppgaven er å etablere en numerisk modell i stand til å modellere kombinert infiltrasjon og overvannstrømning gjennom gresskledde vannveier, eller swales. Modellen er tenkt benyttet for å gjøre detaljerte vurderinger av den hydrauliske oppførselen til swales utover tilgjengelige metoder per dags dato.

Det er blitt gjennomført et litteraurstudium, med det resultat at det finnes lite tilgjengelig forskning innen hydraulikk i swales. Selv om det er gjort mye forskning på swales, fokuserer denne forskningen hovedsaklig på vannkvalitet og håndtering av forurensninger gjennom empiriske studier. Dette tyder på at det både er en mangel på, og et behov for, å ytterligere undersøke den hydrauliske oppførselen til swales på et mer detaljert matematisk nivå.

På dette grunnlaget er en numerisk modell som kombinerer eksplisitt løsning av St. Venants ligning for dynamiske bølger med en modifisert Green Ampts infiltrasjonsligning blitt etablert. Dette grunnlaget gjør modellen i stand til å takle varisjoner i strømningsforhold over korte tidssteg. Modellen benytter programmeringsspråket MATLAB og åpner for brukerinput på de mest sentrale modellparametrene. En rekke prøvesimuleringer er blitt gjennomført, på grunnlag av konstruerte data, for å undersøke modellens oppførsel. Modellen gir simuleringresultater som er i tråd med forventet oppførsel ut fra ligningsgrunnlaget. Ustabil modelloppførsel ble påtruffet i tilfeller hvor lave Manningskoeffisienter ble kombinert med høye kanalhelninger, samt når infiltrasjonslaget ble satt til finkornete jordtyper. Det har blitt gjennomført noen forenklinger for å kunne koble sammen modelligningene. Den mest betydelige er innførselen av en kunstig grensevannføring lik $0.005\,m$, i det modellen ikke er i stand til å kjøre stabilt dersom strømningsdybden går mot null. Koblingen mellom ligningsgrunnlaget er årsaken til dette. De hydrauliske ligningene krever meget små tidssteg, hvor infiltrasjonsligningene krever store tidssteg. Dette reduserer spekteret av mulige tidssteg for modellsimuleringen. Dersom korrekt tidssteg legges til grunn, er derimot modellen i stand til å gi konsekvent gode og stabile resultater.

Det er dermed forventet at den numeriske modellen er i stand til å gi resultater som samsvarer godt med reell strømning i swales, gitt tilstrekkelig kalibrering og verifisering. På det tidspunkt denne oppgaven er skrevet er data for slik kalibrering ikke tilgjengelig. Dersom det er behov for å modellere strømning ved tilfeller som nærmer seg null strømningsdybde, anbefales det å utvide til implisitt diskretisering for det hydrauliske modellsteget.

Preface

This thesis is submitted in partial fulfillment of the requirements set for a Master´s Degree in Hydraulic and Environmental Engineering at the Norwegian University of Science and Technology. It contains work from September 2013 to June 2014, and is the work of the author under supervision of Associate Professor Sveinn T. Thorolfsson. The work is based on recent research within the field of urban drainage as well as established hydraulic and hydrological theory. The model which has been established is an adaptation and expansion of a model intended for the hydraulic modeling of a wide river flood wave, given by Professor Nils Reidar Bøe Olsen. Nils Olsen has also provided co-supervision on the model hydraulic step.

While the work in this thesis borders the fields usually considered in overland urban drainage, it has been chosen due to the my view that there is a need for expanding overland drainage beyond hydrology. The work has been immensely rewarding and has expanded my knowledge on the field greatly. While having the facilities for extensive supervision, much care has been taken to write this thesis as individually as possible in order to grant the best possible understanding of the issues in question. It has also been important for me writing a thesis which is not purely theoretical, but also has a practical use beyond this study. While the need for a combined hydraulic infiltration model by itself might be limited, such a model will have much more value if it is expanded into including sedimentation and water quality assessments. This would complement much of the conducted research on swales and in addition reduce the need for costly empirical field studies. This would sadly be too extensive for a Master´s thesis, and it is my opinion that this should be further looked into by others. The model presented in this thesis will, however, form a solid basis for such model extensions.

Lastly I would like to thank my supervisor, Sveinn T. Thorolfsson, for giving excellent guidance and freedom of work. He has been an immensely valuable resource throughout the thesis work, for which I am very thankful.

Contents

List of Figures

List of Tables

1 Introduction

In the world of today there is an ever increasing urbanization. The climate is changing, bringing forth an increased frequency of extreme weather compared to what could be experienced only 20 or so years ago. The combination of these two changing factors are creating issues in urban areas, especially if regard is taken to extreme precipitation. Outdated underground sewer system are experiencing capacity issues. They are in many cases unable of handling the increased runoff resulting from larger rainfall quantities and more impermeable surface area than they were originally designed for. This has lead to a fairly new approach within urban drainage, where the need of bypassing and expanding upon the existing pipe systems has emerged. This has lead to the use of what is often referred to as Sustainable Urban Drainage Systems, or SUDS, where the rainfall events are conveyed and infiltrated on the surface rather than in underground pipes.

This has lead to a division in the scientific areas within urban drainage, where the hydraulics have dominated the pipe systems and hydrology has dominated the above ground systems. While hydrology is a major factor in sustainable urban drainage, ever increasing flooding events show that the hydraulic field cannot be disregarded. The size of floods and their path of conveyance are often erratic and can potentially cause extensive damage to infrastructure. It is therefore important understanding how open flow hydraulics act in urban environments. There has been been developed advanced hydraulic methods for dealing with overland flow recent years, in order to assess the flooding impact in urban areas. These methods are to a large extent purely hydraulic. They will to a very limited extent be able to model the hydraulic response through channels where infiltration is also present, for example swales and grassed filter strips. The result of this is a clear knowledge gap within the hydraulic field in overland urban drainage.

In this thesis an attempt in bridging this gap will be made by establishing a model capable of modeling the effects of infiltration on the hydraulics of overland flow in swales. This model will consist of a hydraulic equation capable of modeling unsteady channel flow for varying conditions, as would be expected in an urban rainfall event. This must then be combined with an infiltration equation which withdraws an infiltrated volume from the channel discharge. This will be calculated numerically using a suitable programming language, on the basis of constructed input data. The scope of this thesis is to establish such a model, which concurs well with the behavior expected from the chosen equations. Sections 2 and 3 are rendered directly from a previous literature study by Grinden (2013), providing the needed background material.

2 Urban Hydrology

2.1 The Impact of Urbanization

In order to fully understand the problems in modern urban drainage, the mechanisms behind urban hydrology and the effect urbanization has had on the hydrological cycle must first be understood. The hydrological cycle can be viewed as a global mechanism on the macro scale, but can also be divided into smaller areas usually defined as specific watersheds. When assessing an urban environment the usual hydrological method is to limit the scale to the natural watershed, or watersheds, the urban environment is established upon.

The process of constructing cities has up to the 1990s been focused of maximizing the available areas for infrastructure. Little or no regard has been taken to take advantage of the infiltration capacity in the natural soils, which has led to a large number of impervious surfaces covering the cityscapes. The effect of this is a significant alteration of the hydrological cycle. Where forested areas, which are normally the subject of city expansion in Nordic countries, can infiltrate up to 50-60 % of the precipitation, dense cityscapes with few pervious surfaces can only infiltrate 10-20 %. If regard is taken to the hydrological water balance in Eq. (2.1), as presented by Dingman (2008), it becomes apparent what the consequences of these changes are.

$$P + G_{in} - (Q + ET + G_{out}) = \Delta S \tag{2.1}$$

In Eq. (2.1) P is precipitation, G_{in} is groundwater inflow including lateral inflow, infiltration and percolation, Q is surface runoff, ET is evapotranspiration, G_{out} is groundwater outflow and $\triangle S$ is the change in water storage. It is apparent that if the groundwater inflow is greatly reduced, the runoff will greatly increase with a constant precipitation. It will also be reasonable to assume that a reduction in pervious surfaces will have some effect of the change in water storage. An increased fraction of asphalt and concrete surfaces will to some extent increase surface ponding after rainfall events, but this will to some degree be offset by an increase in evapotranspiration. The result of this alteration in the hydrological cycle is that flood runoff peaks become larger and reach their peak flow earlier during the rainfall event as shown in Fig. (2.1). This is a reflection of rainfall intensity where most rainfall events are found to have their peak intensity in the beginning of the event. This is however dependent on the local topographical and meteorological factors, but has proven to be a reasonable general assumption. Therefore flash flood incidents are common in large and dense cities where the existing possibilities of rainwater infiltration

are scarce. This is a large area of concern for many cities and is the cause of extensive damages to infrastructure worldwide. In Nordic climates snow melt and snow accumulation will affect infiltration and runoff conditions and must also be taken into account into the hydrological cycle when assessing urban drainage.

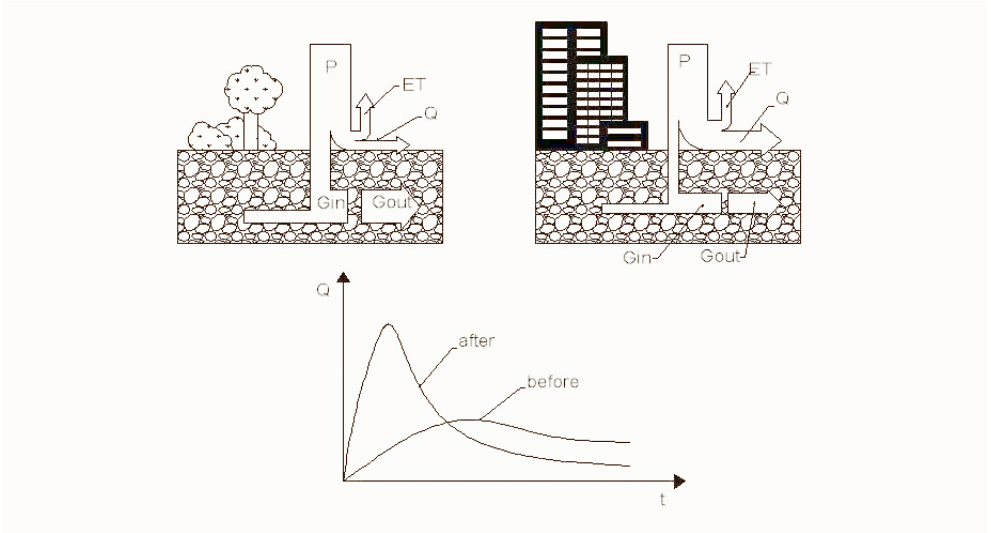

Figure 2.1: The effect of urbanization on the hydrological cycle

Another important effect of urbanization and densification of cities can be seen from Eq. (2.1) if regard is taken to groundwater flow. The natural state of the groundwater flow is that groundwater inflow, consisting of lateral inflow and infiltration, over time will balance the groundwater outflow. This creates a constant mean groundwater table with some small variations linked to the frequency and intensity of rainfall events. If infiltration is greatly reduced by increasing the amount of impervious surfaces, the groundwater outflow will become greater than the groundwater inflow. Gravitational forces combined with capillary forces will then drain the groundwater level to a new, and lower, state of mean equilibrium. This can cause damage to infrastructure and housing due to soil settling. This is a consequence of urbanization that is more hidden than flash flooding, but should be equally avoided.

The main traits of urban hydrology is therefore a reduction in infiltration leading to increased surface runoff and decreased soil water content, again lead-

ing to a lowering of the ground water level. Neither of these effects are desirable and one of the main goals in sustainable urban drainage is to find effective ways of restoring the natural hydrological cycle in dense cityscapes where available areas are scarce. Some care must however be taken in assessing the hydrological cycle on a local scale as there are many uncertainties in hydrological modeling. The driving mechanisms are far more complex than the scope of this project paper, and in order to get a full overview the reader is referred to additional literature.

2.2 The Impact of a Changing Climate

Combined with urbanization and densification of cities, climate changes will also greatly influence the way urban drainage must be understood. It is often said that the global climate is undergoing a change leading to higher global temperatures, melting of polar ice caps and an increase in precipitation volume and intensity. There is to some extent an ongoing debate on the mechanisms behind this change, ranging from a natural long term fluctuation of the global mean temperature to a change caused by man made mechanisms. One of the most widely accepted theories is the atmospheric increase of carbon dioxide due to human activities, where there has been an increase from 280 ppm in 1850 to 353 ppm in 1990 (Dingman 2008). In either way there is an estimated rise in temperature of about 1 to 2 $C^o$by the year 2050, and this will have an impact on the global hydrological cycle. In Nordic climates, which is the area of focus in this project, one consequence could be shorter periods of snowfall and therefore a significant change in the temporal precipitation-runoff balance. There could also be anticipated an increase in evapotranspiration which is driven by temperature. This will lead to an increased amount of water vapor in the atmosphere and therefore giving a potential for intensifying the hydrological cycle with a possible increase in precipitation of 3 % to 15 % with a greater increase at higher altitudes (Dingman 2008).

In regards urban drainage it is important to understand and plan according to a changing global climate. The majority of Nordic urban drainage systems have been planned and built in the 1950s and 1960s when climate and increased runoff was not considered an issue. Combined with urbanization, a changing climate will present problems regarding the capacity of current drainage systems. In order to sufficiently plan urban drainage there is an inherent need for statistical rainfall data. There should be at least 20 to 30 years of daily measurements available in order to establish duration-intensity curves such as the one in Fig. (2.2), which shows an example from the city of Trondheim, Norway.

If climate changes are considered into these curves the statistical basis has to be reevaluated and the uncertainty in rainfall intensity will greatly increase. Therefore not only existing and older urban drainage systems, but also modern systems under planning could suffer from insufficient capacity due to increased precipitation from climatic changes.

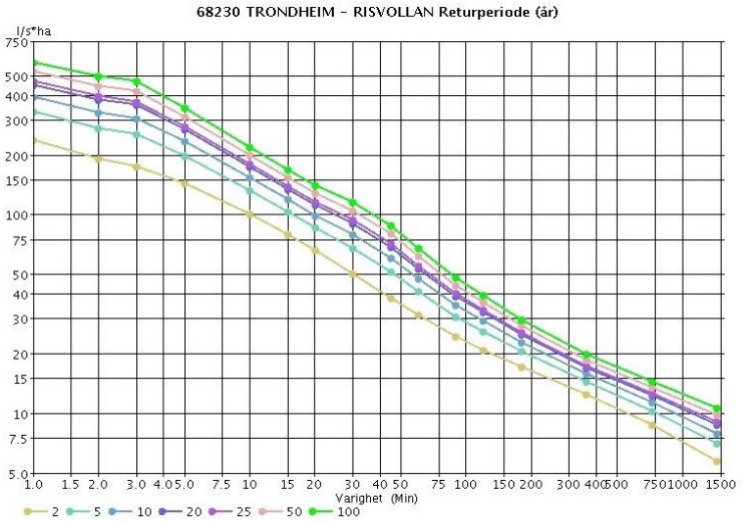

Figure 2.2: Intensity - Duration curve from Risvollan, Trondheim. www.eklima.no, 06.12.2013

How the changing climate will end up influencing urban drainage systems is the subject of a great deal of uncertainties, but it must be taken into account both when assessing existing systems and planning new systems. The main importance is to continually assess the challenges to come and how to cope with them in the best ways possible. With this new line of thought more weight is put on understanding that today's situation is one of change, and that during planning within hydrological and hydraulic engineering this should be kept in mind. There is no doubt that something must be done in the way urban drainage in viewed in general and that moving towards sustainable and robust solutions might be the right way to go.

3 Swales as a Method of SUDS

3.1 General Swale Usage

As mentioned above the rate of urbanization and climatic changes has led to capacity issues for runoff conveyance in traditional pipe based urban drainage systems. There has also emerged a growing concern for the chemical properties of storm water and the effect of these on the biological habitat of the recipients. With these two growing factors it is gradually becoming more and more apparent that a new way of thinking is needed, and that focusing on rapid removal of storm water in not the only priority. The new way of storm water management is centered around sustainable solutions, often referred to as SUDS. These are solutions where the positive effect of storm water can be used to balance out the negative effects such as flooding and pollution of recipients.

One philosophy behind SUDS is presented by Stahre (2006), where solutions for implementation are divided into four sub-categories as shown in Fig. (3.1). The sub-categories are source control, on-site control, slow transport and downstream control. As a whole these groups aim to utilize the natural capacity of the areas in question to infiltrate and retain water, and by these measures counteract the effects of urbanization. The four groups of urban drainage will affect different parts of the urban runoff cycle from small scale upstream watersheds to downstream recipients.

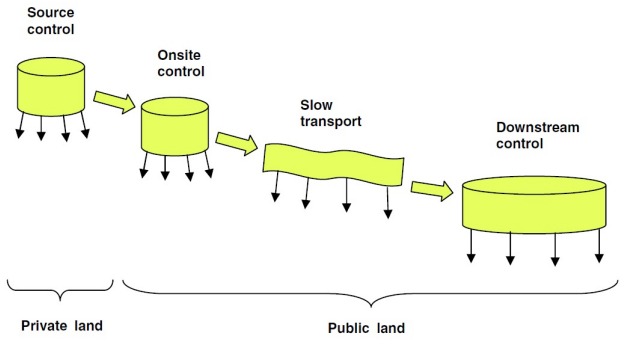

Figure 3.1: SUDS sub-categories (Stahre 2006)

Source control is the smallest scale watershed and is restricted to private land. This group of SUDS will include households, businesses and estates, and

the responsibility of maintaining the systems lies with the land owners. Traditionally this would be the equivalent of gutters leading directly into storm water pipe systems. With an increasing pressure from the municipality to disconnect gutters, the use of SUDS within source control is rising. When considering the on-site control group, these are slightly larger in scale than in the source control group, but cover the same solutions. The responsibility of maintaining and implementing SUDS here lies with the municipality. The group classified as slow transport consists of linking several on-site control systems together and delaying the rapid runoffs which can occur during high intensity rainfall events. This group is the equivalent of the storm water pipe systems that are traditionally used, and are meant as a more robust and sustainable solution. Downstream control is the last of the four groups and consists mainly of detention basins and infiltration solutions to store and improve the quality of large water masses.

When considering swales as a method of implementing SUDS these are normally used for slow transport of storm water and infiltration, and can also be used as a method of source control. In its essence a swale is described as a shallow drainage ditch with flat side slopes (Stahre 2006). A swale has a two part function, both as a flood way for safe conveyance of runoff and as an infiltration bed during smaller rainfall events. Generally swales are used in conjunction with roads as a way of infiltrating runoff from impervious surfaces and safely lead away excess rainfall. This will also to some extent serve as a method for pollutant removal based largely on particle sedimentation. Used in this way as a means of slow transport, swales become large and area consuming in order to be sufficiently effective. The same usage is relevant for source control where the swales lead runoff from impervious surfaces into grassed areas for draining. The need for available area is as mentioned large and limits the use of swales effectively in dense urban areas. In residential areas, however, swales are good alternatives when implementing SUDS. Examples of swales used in different sub-categories are presented in Fig. (3.2).

(a) Swale used as source control (Stahre 2006)

(b) Swale used as slow transport (Stahre 2006)

Figure 3.2: Examples of swale usage

There is also importance in considering the desired effect of swales in Nordic climates, especially during the winter season. In this time of year precipitation falls as snow and is stored in the snow pack. During this season swales are often used as a storage for snow as they are well suited for the task. This regarded in both a positive and negative way in regards to the practical value of snow storage against the increased pollution concentrations and sediment volume that accumulate and the delayed snow melt due to a large snow volume. The negative effects is mainly noticeable during the spring when the thawing process has begun. In this period there is a combination of snow occupying the swale volume, residual frost in the soils and rapid thawing from connecting impervious areas. This presents challenges typical to Nordic climates and must therefore be considered specially when designing swales.

3.2 Swale Design

In general there are not many thorough design criteria for swales in Nordic climates, and for general non-Nordic conditions examples are few. There are however some criteria that have, by experience, proven themselves effective as presented by Stahre (2006), Bäckström (2002) and Leland (2013).

Typically the most common cross-sections used in swales are triangular, parabolic and trapezoidal, where the latter alternative is most commonly accepted as a good design practice. The side slopes should not be steeper than a ratio of 3:1 in order to prevent erosion of the channel sides during high water inflow rates. There is also general agreement in that swale longitudinal slope

design should not exceed 5 ‰, and should typically be in the order of 2 ‰. If this is technically not possible, weirs should be used in order to reduce the water velocity below 1 m/s. This is necessary in order to prevent erosion of the grass and soil layers which, if allowed to happen, will severely impend the swales ability to function as retention of pollutants. The use of grass has proven to be highly resistant to shear forces inhibited by flowing water. The reason for this is that grass roots are dense and keep the top layer of the soil bound. Flow velocities that would usually erode small soil particles will not be able to do this in vegetated due to the stabilizing effect of the roots. The grass will also to a large degree deflect with increasing water depth and velocity, this will further give protection from erosion. At small water depths and velocities the grass will stand erect and provide a substantial resistance to the water flow. As depth and velocity increases during flood events the grass will gradually deflect and provide less resistance to the water flow. In this way the soil layer is protected at the cost of the swales ability to reduce water flow velocity, which in the long term is a desirable effect in order to maintain the swales infiltration capacity. Point sources of inflow to the swales should however be avoided to prevent erosion, as concentrated flow regimes can induce high local friction to the channel section in question. Therefore swales should be designed in such a way that allows continuous inflow along the entire boundary between swale and the adjacent impervious surfaces. In addition there should be an energy break which breaks up super-critical flow conditions of the inflow in order to prevent erosion. Recommended swale design in general is shown in Fig. (3.3).

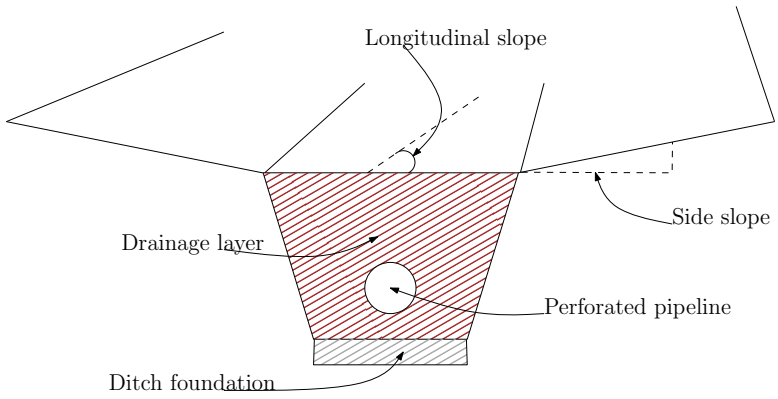

Figure 3.3: General swale design

In swale design, infiltration capacity should also be considered in order to be able to completely infiltrate smaller rainfall events. There are several different parameters which should be considered, but soil porosity and soil water content should be considered the main governing factors. As proposed by Schueler (1987), the soil infiltration rate should be $1.27\,cm/h$ or higher due to the short retention time which is a result of flowing water. Vegetation density should also be considered when designing for infiltration because a dense vegetation cover will limit the infiltration capability of the swale. This must however be considered up against the expected flow conditions and the need for protection again erosion, where a densely packed vegetation will be more resistant to high flow velocities. In addition thought must be given to the ground water conditions to assure that the swale has a large enough storage volume to infiltrate the needed volume of water, for a high ground water level it might be necessary to increase the width of the swale beyond what is recommended when designing for flow conditions. This could be seen in conjunction with the three part strategy for runoff conveyance presented in Norsk Vann report 162 (Lindholm et al. 2008). This design practice is used in Norwegian conditions when dimensioning SUDS for storm water conveyance. As presented in Fig. (3.4), the design practice consists of three parts; complete infiltration of rainfall events $<$ 20 mm, reduction and delay of rainfall events $>$ 20 mm and $<$ 40 mm, and safe conveyance of rainfall events $>$ 40 mm.

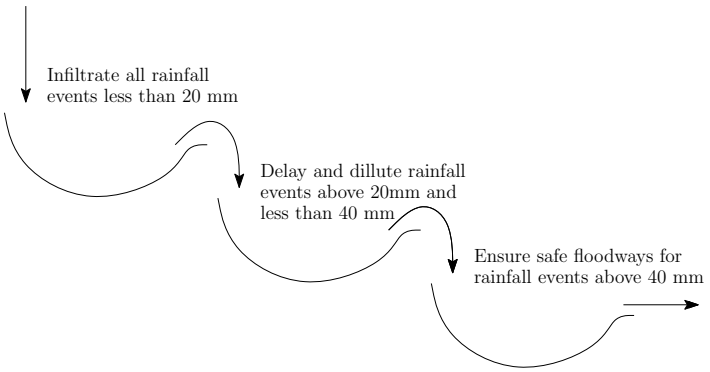

Figure 3.4: Norsk Vann three stage strategy, based on Lindholm et al. (2008)

While the four sub-categories of SUDS can be seen as a classification tool for the choice of methods, the strategy presented by Lindholm et al. (2008) is used more for detailed design criteria. It is therefore important to consider this strategy when designing for infiltration capacity, especially in Nordic conditions. If increased infiltration capacity is needed for very large floods swales could also be designed with a perforated pipeline running the length of the swale with weir intakes positioned at a determined height above the swale bed. The pipeline should be above the ground water level and surrounded by soil with high infiltration capacity. Introduction of a perforated pipeline will also have a protective function during winter conditions in keeping concrete frost from forming (Leland 2013). If the swale is located in conjunction with larger roads or in other areas where a high sediment load could be expected, the reduction in infiltration capacity a resulting of pore filling should be considered.

4 Swale Hydraulics

When planning the use of swales as an implementation of SUDS there are several ways in which this can be approached. Often swales are used in conjunction with moderately to heavily trafficked roads, suburban areas and urban areas. In addition to infiltration and water quality control there is also a certain interest in using swales as a method of safe conveyance and dampening of rainfall events. Therefore the swale hydraulic behavior must be regarded in the planning stage, in order to assess swale capacity and stability. The methods used for hydraulic swale design are, however, in most cases greatly simplified and do not represent the actual physical conditions for most conditions. In this section existing methods, including recent research regarding swale hydraulics, will be presented on a basis of the literature survey conducted by Grinden (2013).

4.1 Commonly Used Swale Design Practice

One of the main methods of hydraulic assessment of swales is the use of empirical research and experience from previously established swales. Design criteria such as these are often referred to as common design practice where key design parameters are given, which are to be followed in order to ensure adequate functionality for design floods. These are methods such as presented by Leland (2013), Lindholm et al. (2008), Stahre (2006), where the hydraulic design parameters are given as recommended longitudinal slope, bottom width and maximum side slope. Flow depth should still be taken into account for the management of maximum flow, and will differ from different geographical locations in such a way that this is not covered in general design criteria and must therefore be assessed using different methods in each case. More detailed design criteria as presented by Leland (2013) also give recommendations regarding the infiltration layer and use of grass covers in order to ensure the desired effect, though this is also on a predominantly empirical basis.

In addition to swale design based on common design criteria, analytical hydraulic equations are also often used. One of the most commonly used is Manning's equation as shown in Eq.(4.1), where Q is runoff (m^3/s), A is cross sectional area (m^2), M is the Manning-Stickler friction coefficient ($m^{1/3}/s$), R is the hydraulic radius (m) and S_0 is the longitudinal channel slope (‰). By implementing Eq. (4.1) for swale flow capacity, water flow velocity and water depth can be found for the case of normal flow in which the flow energy slope is equal to the bed friction slope. In most design situations the inflow to a swale is known and defined by the hydrographs of the corresponding watershed and

the rainfall event which is to be modeled. In such cases corresponding depths can be found by implementing iterative schemes. These will vary in complexity depending on the cross sectional shape of the swale, but will in all cases be rapidly convergent and the use of spreadsheet software such as Microsoft Excel simplifies the process greatly. From a hydraulic design viewpoint the use of analytical equations will give an acceptable approximation of maximum design flow depths corresponding to the inflow hydrographs, which often is sufficient for engineering purposes.

$$Q = M * A * R^{2/3} * \sqrt{S_0} \tag{4.1}$$

Research on the use of analytical formulas has been conducted by Davis et al. (2012), Deletic (2001), Kirby et al. (2005), where empirical studies have found reasonable correlations between analytical formulas and actual observations. There are however some simplifications which are addressed, especially regarding the small flow situations which are to be expected in the initial discharge stage in a rainfall event. In addition to simplifying the slope conditions to assume normal flow depth, analytical formulas such as Eq. (4.1) assume fully turbulent flow conditions, which is defined by a Reynolds number above 10000. The Reynolds number can be computed by Eq.(4.2), and is the product of the flow velocity, U (m/s), the hydraulic radius and the kinematic viscosity,ν (m^2/s). In large scale hydraulics such as river reaches this assumption is valid for most flow conditions. In small scale hydraulics such as can be accoutered in swale hydraulics there is a possibility that the flow regime reaches transitional or near laminar flow conditions, which will create issues with the use of analytical equations. This is especially true to the situation where the flow depth is near the vegetation height in swales.

$$Re = \frac{U * R}{\nu} \tag{4.2}$$

When implementing these methods in real design situations their inaccuracies are often neglected when focus lies with finding the maximum depth and flow situations. This will bypass some of the problems and limitations of the methods which are mostly results of small flow situations. The analytical results will yield design parameters sufficient for capacity design, when including safety factors in order to ensure that overflowing of the banks will be avoided. These methods will, however, not give a detailed picture of the overland flow regime.

Another important aspect of swales is the ability to infiltrate and reduce the rainfall event discharge. This is often neglected in common swale design

where swales are mostly treated as small scale impermeable channels. In the design practice given by Leland (2013) some account has been taken to infiltration by combining infiltration equations with Eq.(4.1). This has resulted in recommendations regarding choice of infiltration media and its thickness, but this method is seldom used in the analytical design of swales. In some way it can be said that the most common design practice in swale design is greatly simplified where the infiltration effect is regarded as a bonus effect. There are however other methods of swale design, which are not as commonly used, but do address some of these issues.

4.2 Advanced Swale Design Practice

While the most commonly used design practice presented in the previous section mainly relies on experience and analytical formulas, there are some more advanced methods of swale design available. Most of these are in the form of computational software which to some extent is able to make better mathematical representations of the physical flow conditions. The way in which these models are better suited than the use of analytical solutions, is foremost the ability to better model overland flow conditions. Software such as HEC-RAS and Mike Urban are able to model 1D and 2D fully dynamic overland flow. The improvement in these models are that the dampening effect of the channel roughness is taken into account in order to make a better assessment of the swales ability to delay and reduce maximum discharges. Both these software implement the St. Venant´s equation, which will be presented thoroughly in Section 5. On the other side this software is strictly limited to overland flow, and will not be able to model the infiltration behavior of swales. Their usage is therefore limited in detailed hydraulic swale assessments.

Another software, which includes a swale module, is PCSWMM. In addition to modeling pipe flow and rain gardens there is also an option to model swales specifically. The mathematical basis is, however, very simplified by implementing Manning's equation for overland flow and Hortons infiltration equation. The same limitations as for analytical solutions are thereby present, but the software engine makes computations much faster and less time consuming than using spreadsheet calculations. It is therefore a valid method of a somewhat simplified practice. Yet this is the most advanced readily available method of swale design and would be sufficient for most engineering applications.

4.3 Hydraulic Research on Swales

In addition to the already established methods of swale hydraulic design, there has been an increase in research conducted on the subject of swales in recent years. While most of swale research in focused on water quality control and pollutant management (Bouchard et al. 2013, Hood et al. 2013, Lantin and Member 2005, Muthanna et al. 2007, Pitt et al. 2008, Stagge et al. 2012), some research regarding hydraulic aspects related to swales has emerged. These researches by Naot et al. (1996) andGilliam et al. (1999) are mainly focused on small flows through grass filter strips, which in its essence is a simplified form of channel flow where the hydraulic radius can be replaced with the water depth for simplified calculations. The research conducted by Gilliam et al. (1999) is the most relevant research when considering swale research on hydraulics. In the model developed in this research there are three stages; the first stage is an unsteady flow equation, the second in an infiltration step, and the third is a sedimentation step in order to assess water quality impact. If the model is considered to be valid for the hydraulic response of swales the first two stages are especially interesting. In the way that introducing dependency on the cross sectional shape by implementing the hydraulic radius the model could be directly translated to a combined swale discharge - infiltration model.

The model in question implements the kinematic wave equation given by Eq. (4.3)

$$\frac{\partial h}{\partial t} + \frac{\partial q}{\partial x} = i_e(t) = r(t) - f(t) \tag{4.3}$$

where x is the flow direction (m), t is the time step (s), $h(x,t)$ is the mean water depth in a given cross section (m), $q(x,t)$ is the discharge per m width (m^2/s), $i_e(t)$ is rainfall excess yielded as runoff (m/s), $r(t)$ is rainfall intensity (m/s) and $f(t)$ is the infiltration rate (m/s). As can be seen, the kinematic wave equation takes spatial and temporal flow variations into account, while Eq. (4.1) assumes steady state flow. This results in a more accurate representation of a rainfall event in which the inflow will change according to the rainfall intensity over time combined with the catchment properties. There are, however, still limitations in Eq. (4.3) in the way that the energy and friction slopes are still considered equal and acceleration and momentum terms are neglected. While the equation to some extent will be able to model wave behavior in swales, there are still considerable limitations that will be discussed in later sections.

The second stage in the model presented by Gilliam et al. (1999) consists of a modified version of the Green Ampt infiltration equations shown in Eq. (4.4)

and Eq. (4.5)

$$f_p = K_s + \frac{K_s\, M\, S_{av}}{I_p} \tag{4.4}$$

$$K_s(t - t_p + t_0) = I - M\, S_{av}\, ln(1 + \frac{I}{M\, S_{av}}) \tag{4.5}$$

where f_p is the infiltration capacity for ponded conditions (m/s), K_s is the saturated vertical hydraulic conductivity (m/s), M is the initial soil water content (m^3/m^3), S_{av} is the average suction across the wetting front (m), I_p is the cumulative infiltration after ponding (m), I is the cumulative infiltration for the event (m), t is the actual time (s), t_p is the time of ponding and t_0 is the correction for not having ponded conditions at the start of the event. In each computational step Eq. (4.3) and Eq. (4.5) are combined in order to evaluate infiltrated volume and excess rainfall as discharge. The implementation of these equations makes the model capable of handling unsteady conditions for both discharge and infiltration, giving a better alternative to swale modeling than established methods.

4.4 Weaknesses Within Existing Methods

Even though the methods of hydraulic swale modeling described within this section are sufficient for most engineering purposes, there are limitations when more detailed investigations are to be conducted. As there is much ongoing research on the effects swales have on pollutant control, a need has risen for a better understanding of swale hydraulic properties. Nearly all of this research is based on empirical data which to some extent is limited for the specific research location and swale configuration, making extrapolation of data the only way of predicting the behavior of swales in general. This methodology might be sufficient for calculating estimates, but there are numerous approximations which must be made. From a research viewpoint this is commonly regarded as bad practice, which leads to a certain interest establishing a physical-mathematical model able to accurately represent swale flow, infiltration and sedimentation behavior. It is in this respect especially the hydraulic stage in most existing swale modeling methods is lacking in detail. While the research presented by Gilliam et al. (1999) presents a major step in swale hydraulics, there are still limitations which need to be addressed.

As mentioned in Section 4.1 there are significant simplifications in using Manning´s equation for hydraulic swale calculations. The most substantial

simplification is the assumption of the water flow energy slope, S_0, being equal to the bed friction slope, S_f, yielding normal flow conditions. These conditions can appear in natural channels, but require long and uniform geometry combined with constant discharge conditions on order to for the flow to stabilize. In real swale conditions short term hydrographs are used, which combined with fairly short swale lengths makes it unreasonable assuming such conditions occurring. In addition to the assumption of normal flow conditions there are several other simplifications in using Manning´s equation that must be regarded. These are focused on the dampening and retarding effects the channel bed roughness will have on the flow conditions. These are disregarded completely which will lead to a outflow hydrograph being identical to the inflow hydrograph just being displaced spatially and temporally. This can be graphically represented as seen in the time - discharge diagrams in Fig. (4.1).

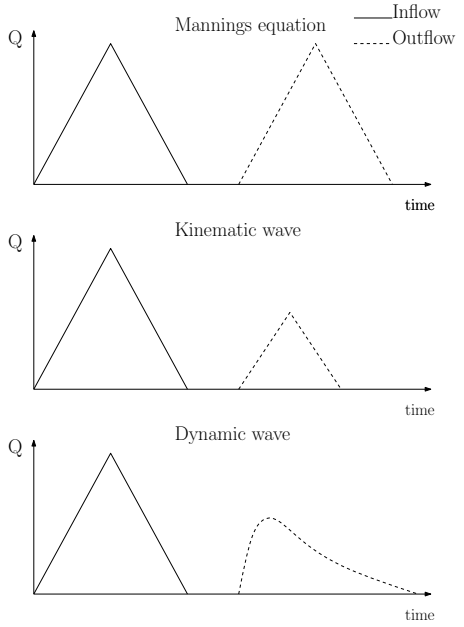

Figure 4.1: Comparison hydraulic equations

To confer with field observations one would expect a certain retarding effect due to bed friction, which is one of the benefits of implementing solutions such

as swales in urban drainage. When implementing the kinematic wave equations shown in Eq. (4.3) some dampening is introduced on a basis of time dependent steps in calculations based on friction equations such as Manning´s formula. By still making this assumption, the flow depth will be a unique function of the discharge. For observed field conditions this will not be the case due to differences in water velocity for a given discharge depending on whether the wave is rising or falling. This can be seen in the rating curve shown in Fig. (4.2) where a single discharge value can result in two different water depths. Since the kinematic equation assumes normal flow it will not be able to model these observations. One must also take into account artificial dampening effects which can occur by solving the kinematic wave equation by differentials. These are due to inaccuracies in the differential scheme and must not be confused with real field dampening (Olsen 2011). In some ways this is an improvement on established methods, but the dampening effect and rating curve should improved upon. This is especially important for small scale flows where friction forces are more dominating than in large river reaches and therefore will have a larger relative effect on modeling results.

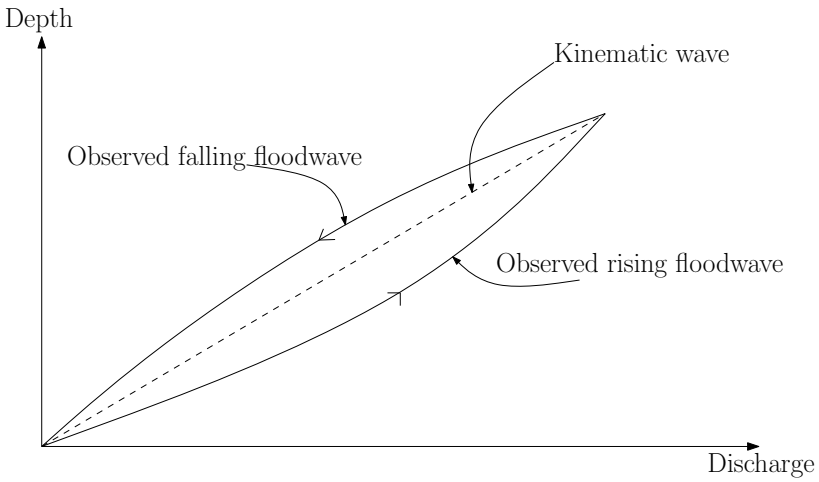

Figure 4.2: Kinematic wave rating curve, based on Olsen (2011)

In order to model overland flow, such as can be observed in field data, there is a clear need of improving the mathematical foundation in order to better the inaccuracies presented by the kinematic wave equation. Experience can be taken

from softwares such as HEC-RAS and Mike Urban, where the implementation of fully dynamic wave equations have proven themselves more than adequate in recreating field measurement data. In this thesis a model implementing St. Venant´s equations for dynamic flow, where friction slopes and energy slopes are treated separately and momentum and acceleration terms are introduced, combined with infiltration equations will be introduced.

When considering the infiltration step, a similar approach to that of Gilliam et al. (1999) will be taken, implementing a modified Green Ampt infiltration equation for ponded conditions. In general, infiltration equations are results of empirical work and will therefore at best be semi-empirical by nature. The two leading equations are Horton´s equation as utilized by PCSWMM, and Green Ampt's equation. The advantage of using Green Ampt's equation is that initial soil water saturation is taken into account. This will be of practical use in a swale hydraulic modeling scenario in the way different saturations are to be expected due to variations in time and weather between rainfall events. Combining St. Venant´s equation for overland flow and Green Ampt's equation for infiltration will yield a physical - empirical model with a combined capacity of modeling water conveyance through swales through a range of rainfall events. The mathematical foundations and numerical implementations will be presented further in sections 5 and 6.

5 Model Governing Equations

5.1 St. Venant´s Equation

As mentioned in Section 4.4 it is necessary to implement dynamic wave equations in order to accurately model and describe the impact of bed friction and momentum forces in swale hydraulics. One the most established equations capable of describing these physical parameters are the previously mentioned St. Venant´s equation, which is derived from Newton´s second law and often combined with a continuity equation to calculate flow conditions (Olsen 2011). Although a derivation of the equations is given by Olsen (2011), a presentation of the equation terms will be given in this section in order to order to give the reader a comprehensive overview of the mathematical foundation of the swale model established in this thesis.

The St. Venant´s equation is in its most basic form is a summation of all the forces acting on a volume of water traveling along a sloped surface. This can be described by Newton´s second law as shown in Eq. (5.1), making the St. Venant´s equation a mathematical - physical equation set, where the sum of forces on the water volume is equal to its mass, m, times acceleration, a.

$$\sum F = ma \tag{5.1}$$

If a control volume approach over a given spatial time step, Δx, is given according to Fig. (5.1) the right hand side of Eq. (5.1) can be described in Eq. (5.2) as

$$ma = \rho y B \Delta x \frac{\partial U}{\partial t} \tag{5.2}$$

for rectangular cross sections where ρ is the water density (kg/m^3), y is the upstream water depth (m), B is the channel width (m) and $\frac{\partial U}{\partial t}$ is the change in velocity as the flow propagates through the reach (m/s^2). While this is given for rectangular cross sections in this section, the same will be valid for different shaped channel cross sections but yield more complex expressions for the mass term. In this section all equations will therefore be given for rectangular cross sections.

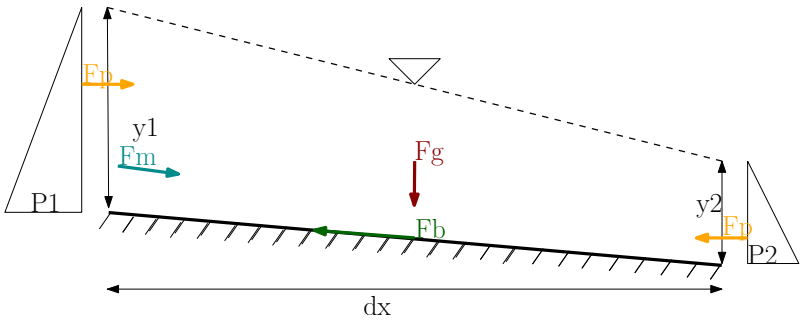

Figure 5.1: St. Venant forces, based on Olsen (2011)

The left hand side of Eq. (5.1) is the sum of external forces acting on the control volume, which can be summed up to four terms; the gravity term, the bed friction term, the pressure term, and the momentum term. Together these terms cover all major forces determining the flow propagation. The first term to be presented is the gravitational term, induced by the control volume mass, shown in Eq. (5.3) which is the main driving force for the flow.

$$F_g = \rho g y B \Delta x S_0 \tag{5.3}$$

Here S_0 denotes the channel longitudinal energy slope (‰) and yields the force from friction free runoff along an inclined slope. Note that S_0 is the dry bed slope as used in Eq. (4.1). While simplified hydraulic calculations assume a constant roughness coefficient to be coupled with the dry bed slope, this will in field conditions change according to flow depth and velocity. In order to take into account these changes the bed friction term is included separately in St. Venant´s equation through Eq. (5.4).

$$F_b = -\rho g y B \Delta x S_f \tag{5.4}$$

In Eq. (5.4) the bed friction slope is estimated through empirical roughness equations such as Eq. (4.1). While S_0 is a constant coupled to the bed slope in the hydraulic reach in question, S_f will vary depending on the actual flow depth and velocity in the same reach. Only if the actual flow depth is equal to the normal flow depth will S_f be equal to S_0, thus fulfilling the assumptions made in Eq. (4.1) and Eq. (4.3). For all other flow conditions the slope will not be equal to each other and must therefore be treated separately. Note that

the bed friction term is negative due to the fluid flow direction being defined as the positive direction.

When modeling unsteady flow conditions, discharge and therefore also fluid levels, will change over time. In short term events where flow changes are fairly rapid such as often can be found in urban drainage situations, care must also be taken to variations in water depth over a control volume. As a wave is either rising of falling there will be a certain difference in depth in the upstream and downstream boundary, inducing pressure gradients on the flow. The third term in the St. Venant´s equation, as shown in Eq. (5.5) presents this as

$$F_p = -\rho g B y (\frac{\partial y}{\partial x} \Delta x) \tag{5.5}$$

where $\frac{\partial y}{\partial x}$ is the change in depth from the inflow boundary to the outflow boundary of the control volume. The resulting force is due to the different hydrostatic pressures in each boundary and will either accelerate or decelerate the flow. If the inflow depth is greater than the outflow depth, giving a rising wave front, the pressure will accelerate the flow due to a negative $\frac{\partial y}{\partial x}$. If the situation opposite, a falling flood wave, there will be an opposite effect. Note that Eq. (5.5) is defined negative, which is due to the upward gradient being defined as positive. In order to correct the pressure term for the behavior of rising and falling waves it must therefore be set negative.

The final term of St. Venant´s equation handles the mass flow momentum forces. The momentum is dependent on the change in velocity gradient over the control volume reach as shown in Eq. (5.6).

$$F_m = -\rho U B y \frac{\partial U}{\partial x} \Delta x \tag{5.6}$$

Here U denotes the upstream boundary velocity of the control volume (m/s) and $\frac{\partial U}{\partial x}$ is the change in velocity over the reach (m/s^2). If the velocity is increasing over the control volume, the momentum leaving the control volume will be greater than the momentum entering the control volume. This will in turn result in a negative force along the positive flow direction thereby yielding a negative sign. This will correct itself according to situations of rising or falling flood waves in the same way as Eq. (5.5).

By substituting Eq. (5.2) to Eq. (5.6) into Eq. (5.1) and simplifying by $\rho g y B \Delta x$, St. Venant´s equation for fully dynamic flow emerges.

$$g(S_0 - S_f) - g(\frac{\partial y}{\partial x}) = U \frac{\partial U}{\partial x} + \frac{\partial U}{\partial t} \tag{5.7}$$

Note that Eq. (5.7) is independent of cross sectional shape in the way that $\rho g y B \Delta x$ denotes all parameters for mass and geometrical calculations, and will be the same for all terms within different cross sections. Therefore the St. Venant´s equation itself can be viewed separate from cross sectional geometry inn all terms except for S_f, which is estimated through external friction equations where the hydraulic radius must be taken into account. However geometry can not be disregarded in the remaining terms as it is needed in calculating estimates of velocity and depth gradients. When calculating flow parameters other equations are needed in combination with Eq. (5.7), and a continuity equation is often implemented. The essence of a continuity equation is that the changes in discharge due to rising and falling water depths must be equal to the amount of water conveyed through the same reach. As presented by Olsen (2011), this can be seen by regarding the change of volume, ΔV, while considering a control volume approach. The change in volume can viewed both as the inflow and outflow through the control volume during a time step, Eq. (5.8), and the change as a result of rising and falling water levels combined with change in cross sectional area, Eq. (5.9).

$$\Delta V = -\frac{\partial Q}{\partial x}\Delta x \Delta t \tag{5.8}$$

$$\Delta V = \frac{\partial A}{\partial t}\Delta x \Delta t \tag{5.9}$$

Here the positive direction is defined as a decrease in water depth and discharge over the reach, explaining the negative sign in Eq. (5.8). Since the change in volume must be constant over the same reach for the same spatial and temporal step the continuity equation, Eq. (5.10), is given by combining Eq. (5.8) and Eq. (5.9).

$$\frac{\partial A}{\partial t} + \frac{\partial Q}{\partial x} = 0 \tag{5.10}$$

From the continuity equation depth and velocity can be estimated from initial conditions by discretizing the terms. These estimates will take into account geometrical factors and inflow discharge, making it possible to calculate Eq. (5.7) with given geometrical factors from external equations. The estimates from Eq. (5.10) are fed into the St. Venant´s equation where the estimates are corrected by solving all differential terms in order to take the physical forces into account. This will yield depth, velocity and discharge parameters which are accurately representative of field conditions. It must, however, be made clear

that the resulting accuracy of Eq. (5.7) combined with Eq. (5.10) is greatly dependent on the numerical scheme chosen to discretize them since they can not be solved analytically. This will be discussed further in Section 6.

5.2 Green Ampt´s Equation

While St. Venant´s equation is based on physical-mathematical considerations, the infiltration process is often based on empirical studies. The reason for this is that the infiltration media, or matrix, is often inhomogeneous with a fair amount of uncertainties regarding the composition and physical properties, making describing water flow through it very complex. Therefore empirically based equations have been thoroughly investigated in order to simplify the calculations needed, where some of these have become well established within engineering. One of these equations, which has proven itself capable of modeling infiltration consistently with field results, is Green Ampt´s equation for unsteady inflow conditions. Green Ampt´s equation is derived from Darcy´s law, Eq. (5.11), which is based on conservation of momentum of fluid flow through a homogeneous matrix.

$$Q = \frac{-kA}{\mu} * \frac{\triangle p}{L} \tag{5.11}$$

Here Q is the discharge (m^3/s), A is the area normal to the flow direction (m^2), L is the matrix length in the flow direction (m), μ is the fluid viscosity $(Pa*s)$, k is the matrix permeability (m^2), and Δp is the total pressure loss over the matrix (Pa). This is valid for constant conditions and a homogeneous matrix in saturated conditions. For real life infiltration purposes these conditions are seldom fulfilled, making it necessary adapting Darcy´s law for conditions with varying inflow and matrix saturation levels. There are several equations used for this purpose, and Green Ampt´s infiltration equation is often used due to its ability to take into account varying matrix saturation in order to calculate infiltration rate.

Green Ampt´s equation considers only flow in the vertical direction for non-sloping surfaces, which is not the case in swale infiltration. In a study by Chen and Young (2006), Green Ampt´s equation has been modified to include a sloping surface, yielding Eq. (5.12), describing the cumulative infiltration over an infiltration event.

$$I = K_{sat} * t * cos(\gamma) + \frac{(\psi + y * cos(\gamma))(\theta_{sat} - \theta_i)}{cos(\gamma)} \\ *ln[1 + \frac{I * cos(\gamma)}{(\psi + y * cos(\gamma))(\theta_{sat} - \theta_i)}] \tag{5.12}$$

Here I denotes the cumulative infiltration (cm), K_{sat} is the effective saturated hydraulic conductivity (cm/h), t is the duration of the infiltration event (h), γ is the longitudinal slope angle (rad), ψ is the wetting front matrix suction potential (cm), y is the overland flow depth (cm), θ_{sat} is the saturated volumetric water content (cm^3/cm^3) and θ_i is the initial volumetric water content (cm^3/cm^3). The empirical aspect of Eq. (5.12) shows through the constants K_e, ψ and θ_{sat} which are empirical values set constant throughout the calculations. These are often found for typical soil conditions experimentally, and established tables are readily available such as the widely used soil water properties presented by Rawls et al. (1982). The cumulative infiltration is then corrected taking into account the added suction for non-saturated conditions and the increase in soil saturation as the cumulative infiltration increases, represented by the second term on the right hand side. The first term on the right hand side represents flow in saturated conditions described by an empirical hydraulic conductivity thereby representing Darcy´s law.

The use of experimental values in describing soil conditions poses a simplification requiring a fairly homogeneous soil matrix, which has proven itself difficult achieving in field conditions. This is however often regarded to be an acceptable approximation to field conditions. Describing and calculating the flow trough a matrix exactly from a physical view would yield complex calculations beyond what is reasonable in engineering purposes. By adjusting saturation levels as an increasing amount of water is infiltrated, a fairly accurate approximation to field observed data is given. It must also be noted that the Green Ampt´s equation assumes a constant wetting front with a instantaneous change in saturation from saturated conditions above the wetting front depth to partially saturated conditions below, Fig. (5.2). In an actual infiltration event it should be noted that the saturation conditions vil change more gradually. For large time step calculations this approximation could yield errors which are significant to the results, but for smaller time steps the equation becomes more accurate.

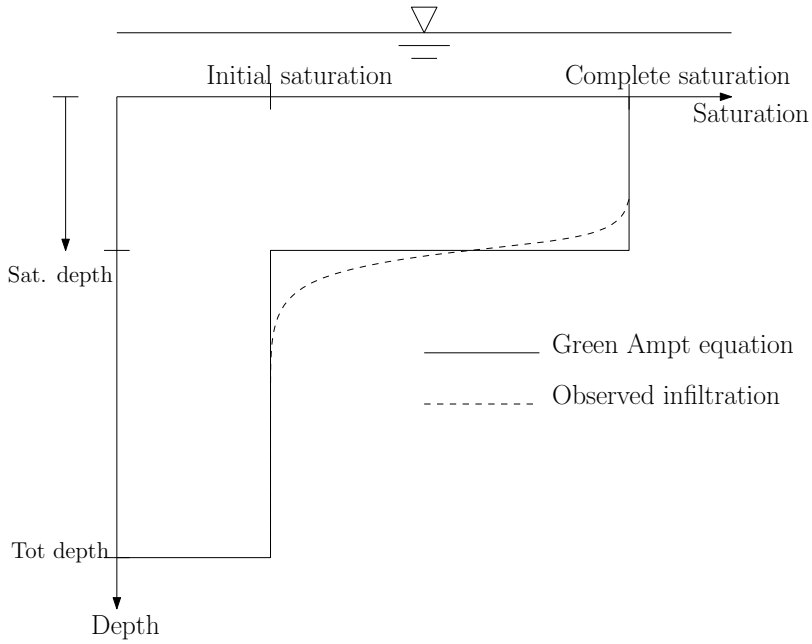

Figure 5.2: Green Ampt infiltration approximations, based on Dingman (2008)

In addition to the simplifications of an empirical equation, the inclusion of sloped conditions must be discussed. In the study by Chen and Young (2006) the slope of the surface is taken into account by adding a factor of $cos(\gamma)$ to the calculation terms. For small slopes this will calculate to a factor of near 1, not making a significant impact on the result as compared to horizontal conditions. When investigating the effect of the slope factor it was found that above an angle of around 10 degrees results would start to differ significantly. While swales often have very low longitudinal slopes, it is seen as beneficiary to include the slope in order to explore outer limits of swale design when regarding erosion control in order to reflect the setup of the over and flow equations. From the study it was also found that an increase of the slope will effectively increase the infiltration longitudinal length leading to greater infiltration volumes as compared with regular Green Ampt´s infiltration. On this basis Eq. (5.12) for ponded sloping conditions will be adequate in calculating swale infiltration. Due to the inclusion of sloping conditions it must be noted that the infiltrated depth is normal to the sloping surface and not vertical as is the case in Green

Ampt´s equation for non-sloping surfaces.

It must also be noted that the corrective term for not having saturated conditions is dependent on the cumulative infiltration in such a way that the result of the equation is dependent on itself as can be seen in Eq. (5.12). When calculating the cumulative infiltration an initial value of I must be guessed and the equation must be iterated to the point where I is equal on the right hand and left hand side of Eq. (5.12). There is however still a weakness in that volumetric distribution of cumulative infiltration and saturation conditions are assumed uniformly distributed along the longitudinal flow with all calculations taking place in the vertical direction. In a swale modeling approach this must be handled by numerical schemes taking into account the calculation time step and wetted length of the swale. This will be discussed further in Section 6.

6 Modeling Method

When establishing a numerical model there are several considerations that must be made in order to compute the equations presented in Section 5 accurately and efficiently. There are several different approaches which could be taken, yielding varying degrees of accuracy. In this thesis a one dimensional model has been established in the MATLAB programming language, implementing an explicit solver for the overland flow equations and an implicit solver for the infiltration equation. This has in result yielded a semi-implicit, semi-physical model designed for estimating swale flow and infiltration regimes.

6.1 Choice of Programming Language

One of the first steps of establishing a numerical model is the choice of software and programming language which is suited for the required calculations. While there are many possibilities, the most important aspect is the flexibility and computational power behind the program. Depending on the desired dimensional model build up, different languages could be preferred. In the model developed in this thesis the numerical solvers require a high number of iterations in order to yield accurate results. It is also beneficiary to have the flexibility to solve the necessary equations in vectors or matrices in order to better take into account factors such as changes in cross sectional geometry and other significant parameters. While several programming languages such as MATLAB, C++, C and Fortran are widely used within numerical computations, MATLAB has been chosen in this thesis. MATLAB is widely used within civil engineering and is the most widely used programming language at the Norwegian University of Science and Technology, making it a natural choice. Another point at which MATLAB excels is the ability to compute equations symbolically in addition to numerically. While the model in this thesis is inherently numerical by nature, there are some modeling steps in which a symbolic approach could be beneficiary. The MATLAB language, while not having a graphical interface, has powerful capabilities regarding graphical representation of data making it well suited for the model in this thesis.

6.2 Model Dimensions

6.2.1 Hydraulic Step

When establishing a model describing the hydraulic behavior of a water mass in general, one must first consider the flow regime which could be expected in

field conditions. There must, for example, be taken different approaches for well defined channel flows as opposed to the flow which could be expected on a flood plain. The main question in such circumstances would be to which degree certain flow directions could be considered as dominating while others could be neglected. If the flow regime is not modeled in three dimensions implementing equations which accurately describe complex hydraulic behaviors, there will always be approximations in the modeling situation when compared to field conditions. The approach chosen then becomes a question of what is acceptable in terms of accuracy and scale compared to field conditions. This is often a trade off between desired accuracy for the purpose in question and the computational resources needed for running the model. In many instances accuracy will be limited by the shear computational power needed, where technological advances will lead to greater modeling possibilities.

When considering swales specifically in the process of establishing a numerical model, an assessment of swale hydraulic behavior must be made. In most cases swale flow is closely related to flow in a straight channel where the dominating flow is in the longitudinal direction of the swale. There is, however, one significant difference in swale flow regimes when compared to channel flow. While channel flow has clearly defined inflow and outflow points, the inflow conditions in swales can rarely be defined as a single point. Swales are mainly used in conjunction with roads and in urban areas as method of drainage from impermeable surfaces. This often leads to inflow conditions consisting of continuous inflow from the swale circumference as illustrated in Fig. (6.1). In field conditions this is a desired effect in order to reduce the risk of erosion due to concentrated inflow points (Leland 2013). This will however make describing flow conditions in a numerical model complex due to the initial assumption that several flow directions are in need of being modeled. In addition this will yield difficulties in defining the boundary conditions needed for the model to run properly.

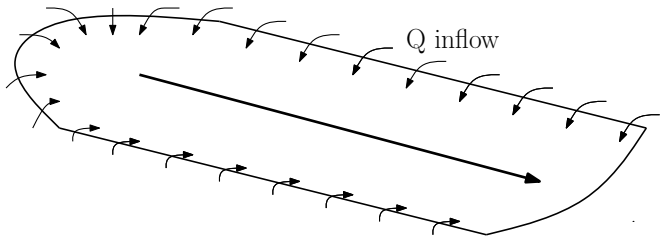

Figure 6.1: Swale inflow conditions

This leads to the discussion of dominating flow directions and the desired accuracy of the numerical model which is to be established. While the inflow in many cases will be oriented laterally relative to the swale length direction, these flows are often far smaller than the channel longitudinal flow which is composed of the cumulative sum of lateral inflows. While this difference might be insignificant in upper parts of the swale, it becomes more significant as the longitudinal flow moves through the swale. This will in many rainfall events lead to flow depths in the longitudinal direction in the order of tens of centimeters while the lateral inflow could be in the order of one centimeter. In conditions as these, the lateral inflow will have very little effect on the longitudinal flow other than adding to the volume of the flow. Investigating the relation between longitudinal and lateral flows in such cases would require powerful physical equations and extensive computational resources. In this thesis investigations are to be made on how infiltration affects the channel flow. This would lead the computation of lateral flows to occupy a large amount of the data power needed in order to run simulations, without giving a significantly added accuracy of the results. Taking the approach of modeling this relation would also require more advanced equations than St. Venant´s equation with the capability of modeling eddies, making a two dimensional approach beyond the scope of this thesis.

6.2.2 Infiltration Step

While the overland flow is defined by the relative relation between flow directions, the same can not be said for the infiltration step. In this step consideration is taken to the inflow flux into the channel bed and through the soil matrix. While overland flow is driven by gravity and viscosity, the flow through a soil matrix is in addition greatly dependent on soil properties such as porosity, pore structure and the resulting suction forces. In this case the driving forces are more equal relative to each other making it difficult defining dominating

directions. In this case more attention must be devoted to the nature of the empirical equations implemented in the model.

In this thesis Green Ampt´s equation has been chosen due to its ability to take into account initial soil moisture content and cumulative infiltration with consistent results compared with field research. This equation treats infiltration as a one dimensional flux in the vertical direction. In this thesis the modification done by Chen and Young (2006) corrects this for sloping surfaces in such a way that the infiltration direction is normal to the channel bed slope by implementing the factor $cos(\gamma)$. The infiltration is then calculated as infiltrated length given as (cm) and infiltrated volume is then considered as a column propagating downwards through the soil matrix. Taking this consideration is a clear simplification on field conditions in the way that is is expected that the infiltration flux also will disperse the infiltrated water in lateral and longitudinal directions. These are however neglected due to the nature of Green Ampt´s equation. These factors could be modeled on a more physical basis by implementing more substantial infiltration equations, which is something that would require extensive computational power. When making this simplification it must be remembered that there are other factors as well, which also have significant effects of the infiltration flux. In most infiltration models the matrix which is used as an infiltration media is considered homogeneous with an idealized pore structure. In field conditions this is seldom the case, and therefore there must be expected deviations when model results are compared to field tests. If infiltration fluxes were to be assessed in multiple directions, one would also be required to assess the homogenization of the soil matrix in question in order to gain an actual increase in accuracy. The amount of data needed in order to do this is far beyond what would be seen reasonable gathering for a numerical model, making one dimensional modeling sufficient from a practical view. By implementing well established soil parameters such as presented by Rawls et al. (1982), based on standardized soil types, these can be adjusted to sloping conditions by calibrating rather than resorting to multidimensional modeling. In such a way a one dimensional approach for infiltration concurs well with the approach taken to the overland flow, yielding a model with sufficient accuracy for engineering purposes.

When these two steps, which are presented in Section 6.2.1 and Section 6.2.2, are combined a dynamic two step model is the result. While this model in many ways will be much more detailed than what is in general considered as sufficient for engineering purposes, the potential applications of the model must be commented. While the hydraulic design parameters and matrix parameters of a swale might not need to be modeled in such detail, there are other areas

which would benefit of a detailed dynamic approach. As previously mentioned, much of the ongoing research on swales in focused on water quality control. While assessing the effect grassed swales have on this area, empirical studies are often the only available methods. However, with a model yielding detailed hydraulic and infiltration representations capable of accurately replicating field conditions, a strong basis for a mathematical approach to the water quality impact of swales is laid. By expanding the model given in this thesis in ways similar to that of the research conducted by Gilliam et al. (1999) a three part model could be established. While this is beyond the scope of this thesis, it sheds light on the area of interest in which detailed hydraulic swale models are needed. The water quality in a flowing channel is very much dependent on flow conditions in order to assess the degree of sedimentation which will occur. The sedimentation behavior, dependent on flow velocity, and the infiltration will then determine the way in which pollutants are detained. In order to assess these effects one must first establish an accurate model of hydraulics in swales and the impact of the infiltration through the channel bed, which is the scope of the model presented in this thesis.

6.3 Numerical Discretization Schemes

In order to compute the equations needed for the assessment of combined swale overland flow and infiltration, they must be discretized in such a way that in this case MATLAB, can compute the terms numerically. There are two main approaches which can be taken in this discretization process, implicit and explicit schemes. These are most often used separately, but in multiple term differential equations such as St. Venant´s equation a combination of the two methods can be used if sufficient assessments of the effect of such an approach is conducted. The main difference between the two methods is that when using implicit discretization schemes the variable which is to be computed is dependent on itself, while explicit schemes are dependent on variables which are independent of the variable which is to be computed. An example is given by Olsen (2011) when discussing St. Venant´s equation, which can be represented graphically in Fig. (6.2). This example is relevant for all equations in which changes must be regarded both spatially and temporally. As can be seen, the explicit scheme utilizes only the values in the spatial steps $x-1$, x and $x+1$ in the previous temporal step, $t-1$, in order to find the function value in the current spatial and temporal step, (x,t). The calculation of the current steps is thereby based solely on known values already calculated in the previous step. However, in the implicit scheme the spatial values in the current temporal step is also

taken into account. Therefore the function in (x, t) is dependent on $(x-1, t)$, and $(x+1, t)$ in addition to the values in the previous temporal step. The function which is to be calculated in the implicit scheme is therefore dependent on itself and other unknown variables, which clearly shows the difference between the two different schemes.

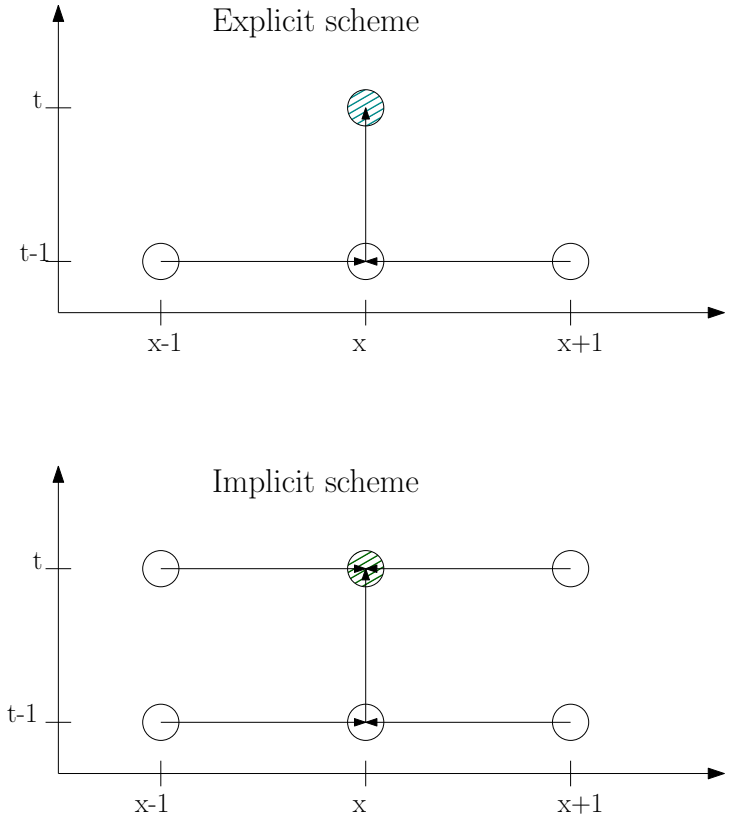

Figure 6.2: Explicit and implicit discretization schemes, based on Olsen (2011)

While the choice between implicit, explicit or combined schemes might not be apparent there are some general differences that could be considered, which are valid for a range of equations. The first aspect that must be evaluated is the complexity behind programming the different schemes. While the explicit scheme in most cases is fairly straight forward to program given proper initial

calculation conditions, the implicit scheme requires a more complex approach. It is often necessary to first establish an explicit estimator and correct these with an implicit corrector. In general implicit solvers will in that way require more computational power and complexity than explicit solvers. On another note this also makes implicit solvers more accurate and stable than explicit solvers, which must often be laid under strict limiters in order to be kept stable. While being more difficult to establish implicit solvers will yield greater accuracy, stability and flexibility, and explicit solvers will require less computational power, and be faster and easier to establish. The choice of which scheme to use must then be considered up against what is to be computed.

6.3.1 St. Venant Discretization Scheme

In order to describe the overland flow in a swale, the St. Venant´s equation, Eq. (5.7), and a continuity equation, Eq. (5.10), must be discretized in order to be able to solve them numerically. When making the choice of which scheme should be used, considerations must be taken to the flow conditions and variations which could be expected in field conditions. Swales are constructed channels built to set requirements and are uniform in the form of sloping conditions and cross sectional geometry. The channel bed is planted with specific grass types and the swales are maintained on a regular basis. In a hydraulic modeling view they are also fairly small and uniform compared to river reaches in natural rivers which are often the subject of hydraulic engineering. Taking this into regard it would be expected that swale flow conditions seldom are the results of rapidly changing external parameters, and that the inflow hydrographs would present the governing parameter for hydraulic variations. The established softwares within river reaches often implement implicit schemes when computing St. Venant´s equation largely for the stability these schemes give regarding to rapid changes in geometry and the resulting risk of instabilities. While this is necessary in river modeling, the same need for the ability is not needed to the same extent in swales where constant frictional and geometrical conditions are to be expected. There is also the benefit of accuracy in using implicit schemes, which might then be the main reason to choose these schemes in hydraulic modeling. The choice must then be made whether the higher accuracy will justify a more complex and resource demanding model.

If regard is taken to the use of explicit schemes these are, as previously mentioned, less table than implicit schemes. In order to keep the models stable, the Courant criteria, Eq. (6.1), is often used as a limiter with the time step as the governing parameter (Olsen 2011).

$$Cr = \frac{U * \Delta t}{\Delta x} \tag{6.1}$$

Implementing an explicit scheme will then require the Courant number, Cr, to have a value less than 1 in order to prevent numerical oscillations. As can be seen in Eq. (6.1) the velocity will be determined by the inflow, cross sectional geometry and friction slope and the spatial step is determined by the channel length. This leaves the reduction of the temporal step the only way to stabilize explicit solutions. If the channel which is to be modeled is long this might lead to a substantial number of calculations needed in order to secure a stable model. To some extent this counteracts the benefits explicit schemes have over implicit schemes in computational demands. In swales, which are typically in the order of hundreds of meters in length, time steps could be kept very small while still maintaining computational speed. Regarding computational speed and stability, the explicit discretization scheme will be an adequate choice for swale hydraulics. The choice then depends on the added accuracy of implicit models. A strictly hydraulic model of swale flow would benefit of using an implicit scheme, especially if more complex cross sectional geometries are taken into consideration. In the model developed in this thesis the hydraulic model is to be combined with an infiltration step utilizing the empirically based Green Ampt´s equation. As a result deviations are to be expected in the infiltration step compared to field measurements, yielding inaccuracies in the model as a sum of both the hydraulic and infiltration step. Therefore the benefit of the increased accuracy from implicit discretization in the hydraulic step would be diminished, making the added computational complexity unnecessary. The computational model in this thesis will thus implement an explicit discretization for the hydraulic step.

Before Eq. (5.7) and Eq. (5.10) can be computed, estimated starting values need to be found from the input hydrograph and will then form the boundary for calculations through continuity and St. Venant´s equations. A friction equation is often used, in this case Manning´s equation, Eq. (4.1). Depending on the cross sectional geometry, the normal depth and velocity can be found by an iterative scheme. This can be set up numerically, where the depth is increased by small steps in each iteration until the control parameters converge within a pre determined threshold. In the iterative schemes used for estimating the normal depth the terms containing the flow depth are gathered on one side of the equation, and the known constant terms are gathered on the other side of the equation. The depth is then increased in the depth dependent terms until they are within a given threshold from the constant terms. There iterative terms

will then become as follows.

$$\frac{Q}{M * \sqrt{S_0}} = A * R^{\frac{2}{3}}$$

$$\frac{Q}{M * \sqrt{S_0}} = \begin{cases} By * \left(\frac{By}{(B+2y)}\right)^{\frac{2}{3}} \\ \left(By + zy^2\right) * \left(\frac{By+zy^2}{\sqrt{B+zy(1+z^2)}}\right)^{\frac{2}{3}} \end{cases} \tag{6.2}$$

In Eq. (6.2) the top alternative denotes the iterative scheme for rectangular cross sections and the bottom is used for trapezoidal cross sections, where z denotes the side slope ($z : 1$). This iterative scheme is widely used and will converge fairly rapidly even with a strict threshold requirement. It is important to set up the schemes with adequate accuracy in order to ensure model stability. If the threshold is set too large the inflow depths estimated by Eq. (6.2) will concur badly with the calculations in the continuity and St. Venant´s equation leading to model errors. This is dependent on inflow conditions with smaller flows being more sensitive, and should be assessed carefully.

When setting up an explicit discretization of the hydraulic step both Eq. (5.7) and Eq. (5.10) need to be discretized, where Eq (5.10) mainly handles geometrical factors and Eq. (5.7) handles the forces acting on the water mass. The geometrical factors are taken as estimations into the St. Venant´s equation where the effect of the forces are calculated. When discretizing the continuity equations, different discretizations must be implemented for different cross sectional geometries and a graphical representation of the computational parameters can be seen in Fig. (6.3). Here the water level in time j is shown in the dashed line and the water level in time $j - 1$ is shown by the dotted line.

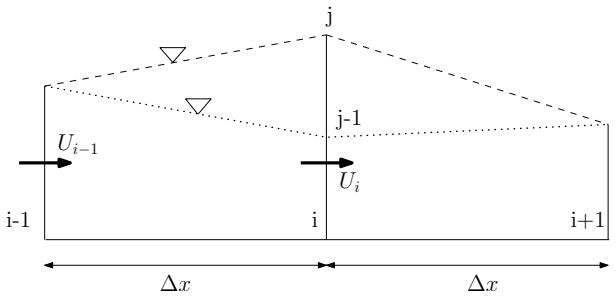

Figure 6.3: Continuity discretization parameters, based on Olsen (2011)

The most basic form of cross sectional geometry is a rectangular channel. The discretization of Eq. (5.10) will then be conducted as follows.

$$\frac{\partial A}{\partial t} + \frac{\partial Q}{\partial x} = 0$$

$$B\frac{\partial y}{\partial t} + U\frac{\partial A}{\partial x} * A\frac{\partial U}{\partial x} = 0$$

$$B\frac{\partial y}{\partial t} + UB\frac{\partial y}{\partial x} * By\frac{\partial U}{\partial x} = 0$$

$$\begin{aligned} B\frac{y_{i,j} - y_{i,j-1}}{\Delta t} + U_{i,j-1}B\frac{y_{i+1,j-1} + y_{i-1,j-1}}{2\Delta x} * \\ y_{i,j-1}B\frac{U_{i+1,j-1} + U_{i-1,j-1}}{2\Delta x} = 0 \end{aligned} \tag{6.3}$$

In Eq. (6.3) the indexing spatial step is denoted by i and the indexing time step is denoted by j, while Δx denotes the spatial distance between each computational step and Δt denotes the duration between each computational step. Note that the swale width, B, remains constant for a rectangular cross sections. Looking more into the discretization in Eq. (6.3) it can be seen that the depth in the current step, (i, j), can be expressed uniformly from computed

values in the previous step, $j-1$, by rearranging Eq. (6.3) in terms of $y_{i,j}$ as shown in Eq. (6.4).

$$y_{i,j} = y_{i,j-1} - \frac{\Delta t}{B} * \left(U_{i,j-1} B \frac{y_{i+1,j-1} + y_{i-1,j-1}}{2\Delta x} * y_{i,j-1} B \frac{U_{i+1,j-1} + U_{i-1,j-1}}{2\Delta x} \right) \tag{6.4}$$

While the model established has the ability of modeling rectangular cross sections, swales will seldom be constructed with such cross sections. This option is mainly intended to make comparisons with calculations for different cross sections in the way that rectangular cross sections have the most stable discretization schemes and therefore serve as good reference points. Most swales have trapezoidal cross sections and are usually designed according to the trapezoidal bottom width and side slope angle (Bäckström 2002, Leland 2013). Therefore the model in this thesis has also been given the capability of modeling trapezoidal cross sections. The discretization of Eq. (5.10) will in this case follow the same procedure as shown above, but will also have to take into account the flow width at the water level in order to assess the cross sectional flow area. The discretization of a trapezoidal cross section can be seen in Eq. (6.5)

$$y_{i,j} = y_{i,j-1} - \frac{2\triangle t}{B + B^t_{i,j-1}} * \left(U_{i,j-1} \frac{B + B^t_{i,j-1}}{2} * \frac{y_{i+1,j-1} + y_{i-1,j-1}}{2\Delta x} \right) * \left(\frac{B + B^t_{i,j-1}}{2} * y_{i,j-1} * \frac{U_{i+1,j-1} + U_{i-1,j-1}}{2\Delta x} \right) \tag{6.5}$$

where B^t denotes the flow width at the water level. In this discretization scheme there has been conducted a slight simplification which should be noted. While expressing the cross sectional areal, $B^t_{i,j}$ in the current temporal step should be used, but it has been set equal to $B^t_{i,j-1}$. This will result in a slightly smaller width than the actual width, and the simplification has been made in order to keep the discretization strictly explicit. It could be discussed whether this is a valid approximation. In regards to the small time steps likely needed by the explicit discretization scheme the change in B^t over one step will be negligible compared to the total width. The approximation is therefore regarded as acceptable in the model presented in this thesis.

In Eq. (6.3) through Eq. (6.5) initial estimations of the depth in the current step is made. In order to compute flow conditions the velocity must then be

computed utilizing an explicit discretization of St. Venant´s equation, Eq. (5.7). The discretization procedure is similar to the process shown above and is given in the following.

$$g(S_0 - S_f) - g(\frac{\partial y}{\partial x}) = U\frac{\partial U}{\partial x} + \frac{\partial U}{\partial t}$$

$$g(S_0 - S_f) - g\frac{y_{i+1,j-1} + y_{i-1,j-1}}{2\Delta x} = U_{i,j-1}\frac{U_{i+1.j-1} + U_{i-1,j-1}}{2\Delta x} + \frac{U_{i,j} - U_{i,j-1}}{\Delta t}$$

$$U_{i,j} = U_{i,j-1} - \Delta t * \left(U_{i,j-1}\frac{U_{i+1,j-1} + U_{i-1,j-1}}{2\Delta x} + g\frac{y_{i+1,j-1} + y_{i-1,j-1}}{2\Delta x} - g(S_0 - S_f)\right) \quad (6.6)$$

In Eq. (6.6) it is thereby clear that the flow velocity can be computed entirely from values calculated in the previous step yielding an explicit discretization. It must also be noted that while S_0 is the given slope for the swale, S_f is dependent on the depth and flow conditions and must be estimated and discretized through a friction equation. In the model presented in this thesis Manning´s friction equation has been chosen, giving an explicit discretization of S_f as shown in Eq. (6.7).

$$S_f = \frac{\mid U_{i,j-1} \mid U_{i,j-1}}{M^{2*} R_{i,j-1}^{\frac{4}{3}}} \quad (6.7)$$

Here the hydraulic radius is determined based on the water depth and corresponding wetted perimeter and cross sectional area in the previous step. These values will be different depending on if a rectangular or trapezoidal cross section is chosen and can be computed on the basis of either Eq. (6.4) or Eq. (6.5).

Combining these equations will yield the necessary values in depth and velocity for each time step and spatial step, and could be repeated in the next step. However, this method will be unstable due to the fact that the depth computed by the continuity equation in Eq. (6.4) or eq. (6.5) does not take into account the forces that have affected the water mass during the computing of the current velocity in Eq. (6.6). Therefore the depth in the current step should be corrected in order to take these factors into account on the basis of the already calculated values in $U_{i,j}$ and $y_{i,j}$. This can be done using an inflow - outflow consideration on the continuity equation where the volume between

the surface in the current and previous step is equal to the difference between inflow and outflow. Taking this consideration, a correction for the depth in the current step can be given as

$$(I - O)\,\Delta t = \frac{1}{2}\,(y_{i,j} - y_{i,j-1})\,2\Delta x$$

$$I = \overline{U}_{i-1} * \overline{y}_{i-1} = \frac{U_{i-1,j-1} + U_{i-1,j}}{2} * \frac{y_{i-1,j-1} + y_{i-1,j}}{2}$$

$$O = \overline{U}_i * \overline{y}_i = \overline{U}_i * \frac{y_{i,j} + y_{i,j-1}}{2}$$

yielding

$$y_{i,j} = \frac{I - y_{i,j-1}\left(\frac{\overline{U}_i}{2} - \frac{\Delta x}{\Delta t}\right)}{\frac{\Delta x}{\Delta t} + \frac{\overline{U}_i}{2}} \tag{6.8}$$

where I denotes the inflow, O denotes outflow and $\overline{U}_i$ is the average computed velocity in the current spatial step. When correcting the depth, $y_{i,j}$, through Eq. (6.8) a significant improvement on stability and accuracy is gained with little loss in computational speed. The discretization approach described above will then give a complete explicit discretization of the model hydraulic step, yielding the desired accuracy and stability.

6.3.2 Green Ampt Iterative Scheme

When considering the calculation process needed to assess the Green Ampt equation, the same discretization approach as is used in the differential hydraulic equations is not needed. When evaluating Eq. (5.12) it becomes clear that while the equation is rooted within the current time step, t. In order to assess the cumulative infiltration, I, it is implicitly dependent on itself. While the depth is known from the hydraulic step, the time is given and all other parameters are known, I becomes the only unknown variable. Therefore a discretization scheme is not needed in the way that the equation can be computed directly. On another hand an iterative scheme is needed in order to find the value for I that will yield an equal value for the right hand side and the left hand side of Eq. (5.12). The iterative process needed is based on trial and error

calculations, making computations time consuming if suitable initial estimations are not given. There are possibilities of modeling Green Ampt´s equation explicitly as given by Salvucci and Enthekhabi (1994), which would result in faster computational times at the cost of calculation errors in the magnitude of 1.5% compared to a well executed iterative solver.

In this thesis an implicit approach has been chosen in order to concur with the constantly ponded sloping conditions and the associated Green Ampt modification as presented by Chen and Young (2006). When conducting numerical computations an iterative scheme must be established by guessing an initial value for the cumulative infiltration and increasing this value until the left and right hand sides converges within a determined threshold value. The Green Ampt equation in the form shown in Eq. (5.12) will converge by this method and the increments in I between each iteration combined with the threshold will determine accuracy and the needed number of iterations. Looking further at Eq. (5.12) it also becomes clear that the time dependent first term on the right hand side, $K_{sat} * t * cos(\gamma)$, is a reasonable initial guess per iteration step rather than starting the iteration process from zero infiltration in each loop.

While MATLAB is mainly intended for numerical calculations there are alternatives when calculating implicit equations such as Eq. (5.12), where a symbolic iteration can be programmed. In the model presented in this thesis possibilities for modeling the infiltration step both numerically and symbolically has been implemented. There are advantages and drawbacks in both methods that the reader should be aware of, which will be presented briefly in the following. While a numerical iteration scheme will rely on an initial value and constant increments in I for each iteration loop until the desired level of convergence is reached, the symbolic scheme relies on a different algorithm. The symbolic solver is a native function to MATLAB where more advanced algorithms introduce variable increments in each iterative step on order to obtain convergence given an initial guess. The cumulative infiltration can then be defined as a symbolic variable which is set to converge in itself. In regards to accuracy this scheme is superior to numerical iterative schemes, and will natively compute convergence with 32 digit accuracy. However, activating symbolic variables demands large amounts of computational power from MATLAB compared to numerical schemes which will iterate faster. One method of reducing the computing time of the symbolic approach is to use MATLAB´s ability to do variable precision arithmetics in which the number of significant decimal accuracy can be altered lower than the native 32 digits. In this model 10 digit accuracy has been defined for the symbolic solver, speeding up the scheme somewhat. It will, however, still be slower than the numerical scheme with the advantage of

increased accuracy. It is up to the user to make the decisions of which scheme is to be used having understood the differences hereby presented.

6.4 Model Build Up

The combined hydraulic and infiltration model of swales presented in this thesis is built up in a fairly linear fashion, which is suitable for the computational schemes given. The model is based upon user input for key computing variables and reads an external inflow hydrograph in the '.txt' format. It consists of three main steps, the first one being an initialization step defining boundary values for overland flow and infiltration which runs only once per model simulation. The two other main steps are hydraulic and infiltration steps which are placed within the main governing loop. In general the model is built up by two nested loops, one controlling the progress in time, j, and one controlling the progress in space, i. The main loop is governed by time, increasing the total time by the user defined time step per loop. Within the main loop, depths and velocities are calculated and corrected for each cross section through the hydraulic equations. This can be seen be seen in the flow chart in Fig. (6.4). While the hydraulic component is calculated in each section, i, for each time step, j, the infiltration step is calculated only once per time step. The spatial dimension in this step is controlled by the wetted length of the swale. This procedure will be discussed further in Section 6.6.

The first computational step of the model consists of the initialization step where the first given discharge in the 'inflow.txt' is read. The normal depth is then computed by Eq. (6.2) belonging to the chosen cross sectional geometry. The normal inflow depth and velocity is then assigned to the spatial steps $i = 1$ through $i = sections + 1$. This will then form the boundary conditions of the model yielding initial reference points for further calculations. In these boundary conditions it is assumed that the model inflow will be of normal depth and velocity according to the inflow hydrograph and that the same is true for an extrapolated constructed cross section at $i = sections + 1$. The same is done for the infiltration step, where an initial infiltration depth is set for the first time step based on the normal depth. The infiltration is only calculated as infiltrated depth and will not add up to the infiltrated volume as it will not form a boundary condition as is necessary for the hydraulic step. In the initialization step vectors for computing depth, velocity, cross sectional area, hydraulic radius and infiltration is set up at the needed dimensions. This will speed up calculations in the main loop by eliminating the need of expanding the vector for each computing step. It must also be mentioned that the vectors

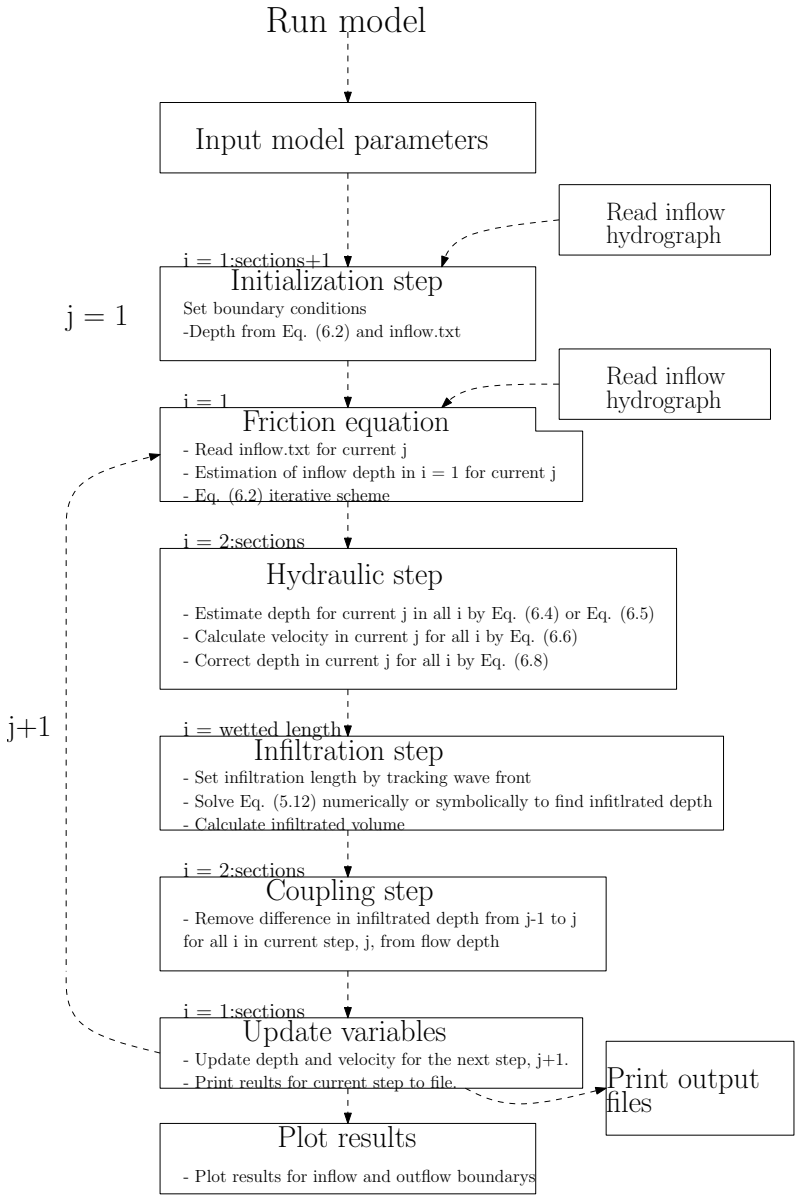

Figure 6.4: Model flow chart

for calculating the hydraulic step is set as a matrix with two columns and rows equal to the number of sections in the given simulation. Each row will then be assigned a time step with the coordinates $(i, 1)$ containing the value for section i in the previous time step, $j-1$, and the coordinates $(i, 2)$ containing the value for section i being computed in the current time step, j. This will then yield a matrix with two columns containing all the values for the relevant parameters for the current and previous time step at each the end of each run of the main loop. The infiltration step is set up as one vector with the length of the number of iterations through the main loop, each space being designated one cumulative infiltration value for the entire time step.

After the initialization step where vectors, matrices and boundary conditions are defined, the main loop is initiated at the first time step. Again inflow is read from the 'inflow.txt' for the corresponding time step where values are interpolated between the values given in the '.txt' file. The initial depth at $i = 1$ is then calculated from Manning´s equation by the same schemes as in the initialization step. For the remaining sections, $i = 2 : sections$, the depth in the current step, $(i, 2)$, is calculated from the depth in the previous step, $(i, 1)$, and Eq. (6.4) or Eq. (6.5) depending on the cross section geometry. When all the depths have been calculated, the velocity in $(i, 2)$ is computed through the St. Venant´s Eq. (6.6) and the depths and velocities in the previous time steps for all sections. The depth is then corrected for $i = 2 : sections$ according to Eq. (6.8) based on the already computed depths and velocities in the current time step, completing one loop of the hydraulic step.

If the infiltration step is to included, it will be initiated after the calculations have run through the hydraulic step. The wetted length in each step will then be computed by tracking the maximum swale flow velocity of the wave front and how far along the channel it has progressed at the current time step. For each main loop run, the cumulative wetted length will be calculated, up to a maximum of the swale length. The cumulative infiltrated depth in the current time step, j, will then be computed by Eq. (5.12) either numerically or symbolically. The difference between the cumulative infiltration in j and $j-1$ is then calculated, which denotes the added infiltration per time step. This is to be subtracted from the flow depth. Depending on the cross sectional geometry the cumulative infiltration is then calculated as volume in (m^3), which is the desired form of results, completing the infiltration step.

The final stage of the model then consists of removing the difference in infiltration between steps from the flow depth, making sure not to remove more water than available. In addition the Courant criteria, Eq. (6.1), is inserted at the end of the main loop and will break the iteration if exceeded. An er-

ror message will then be displayed, in order prevent the need for fully running unstable simulations. The discharge, depth, velocity and cumulative infiltrated volumes are then written into the output files 'Discharge.txt', 'Depth.txt', 'Velocity.txt' and 'Infiltration.txt', yielding the results for the current time step for all sections. The matrices for the hydraulic step are then updated such that the starting values in the next time step will be equal to the computed values in the current time step, meaning $(i, 1) = (i, 2)$. The time is then increased by one time step and the main loop then runs trough the next iteration until the simulation time given by the length of the time step and number of iterations is reached.

When all the runs through the main loop are completed the results for the first, $i = 1$, and last, $i = length/deltax$, sections are plotted for every time, j, yielding four graphical outputs of the simulation. The simulation is then completed and the model will display the text 'Finished!' completing the model run.

6.5 Model Data Requirements

In order to run a simulation of the model presented in this thesis some input data in addition to the 'inflow.txt' file containing an input hydrograph is needed. The model is intended to be very flexible in most modeling aspects, which will require fairly detailed user input. This must be understood by the user. While some of these parameters are self explanatory, others require some knowledge within hydraulic and infiltration modeling. Even though this approach requires more knowledge of the user, it is taken in order to produce a flexible model. Emphasis has still been given to minimize the amount of input needed, and to properly explain acceptable input ranges. The input parameters can be divided into three categories; model governing parameters, geometrical parameters and physical parameters. These parameters are given in Table (1).

Some notes should be taken on some of the input parameters, which might not be apparent to the user. On the first note there is a connection between the time step and the number of iterations which must be understood. The time step will decide the models stability through the Courant criteria, and must be kept sufficiently low. Since the number of iterations determines how many times the main loop will be run, and the time is increased by the time step for each loop, the product of the time step and the number of iterations will determine the total simulation time. It is important that this is sufficiently sized in order to reflect the input hydrograph and the resulting discharge from the swale. Care must therefore be taken to increase or decrease the number of

Input parameter	Range / Comment
MODEL GOVERNING	
Time step	$[s]$
Number of iterations	Assessed from needed simulation time
Swale cross section shape	1 = rectangular, 2 = trapezoidal
Infiltration step activation	1 = yes, 0 = no
Infiltration solver	1 = symbolic, 2 = numerical
GEOMETRICAL	
Swale length	$[m]$
Lengthwise step	$[m]$ Must divide length into equal parts
Lengthwise slope	$[x/1000]$
Bottom width (rectangular and trapezoidal)	$[m]$
Side slope (trapezoidal)	$[x : 1]$
Infiltration media depth	$[cm]$
PHYSICAL	
Manning´s friction coefficient	User evaluated
Soil type	1 = sand, 2 = loamy sand, 3 = sandy loam, 4 = loam, 5 = silt loam, 6 = sandy clay loam
Initial soil saturation	$[cm^3/cm^3]$ Range given for each soil type

Table 1: Model input parameters

iterations accordingly when changes in time step are made.

There are also, as mentioned, parameters which need special considerations from the user. These are grouped as the physical parameters and require individual assessment for each case which is to be modeled. At first there is the Manning´s friction coefficient which must be determined for the grass length and type used in the swale. The availability of of such data is limited on a detailed level and the user must make an initial guess and calibrate according to the field conditions which can be observed. The same is valid for the soil type parameter and the initial saturation. Often natural swales have non-homogeneous infiltration layers and the initial saturation will depend on meteorological conditions, which are subject to a great deal of uncertainties. The user must then guess or measure in each case which choices are the best suited. While there are various ways of deciding soil type matrix properties, the model in this thesis implements well proven empirical values as presented by Rawls et al. (1982). These are shown in Table (2), and are linked to the soil type chosen by user input. This has been done in order to make the model more user friendly and eliminating the need of extensive knowledge within soil water characteristics in order to run simulations.

Soil type	θ_{sat}	θ_{range}	K_{sat}	ψ
Sand	0.437	0.020-0.437	21.00	7.26
Loamy sand	0.437	0.035-0.437	6.11	8.69
Sandy loam	0.453	0.041-0.453	2.59	14.66
Loam	0.463	0.027-0.463	1.32	11.15
Silt loam	0.501	0.015-0.501	0.68	20.76
Sandy clay loam	0.398	0.068-0.398	0.43	28.08

Table 2: Model soil parameters, excerpt from Rawls et al. (1982)

While other governing parameters are all to some extent user defined, the inflow hydrograph must be given in a separate file as stated above. All simulations in this thesis are based on constructed data since there are no available field data for swale hydraulics. A hydrograph, shown in Fig. (6.5), has therefore been constructed in order to represent a typical urban flooding event with a maximum inflow of $600 l/s$, which is a fairly large flooding event. As calibration data becomes available this hydrograph should be updated to match these data. For this thesis this single hydrograph is deemed sufficient to evaluate the model results up against what is expected from the theoretical basis.

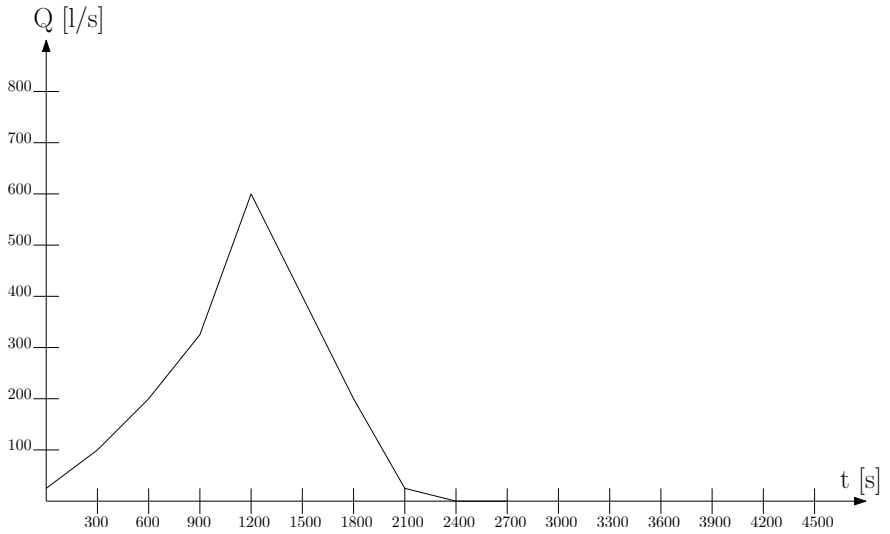

Figure 6.5: Constructed hydrograph

6.6 Coupling Overland Hydraulics and Infiltration

In addition to the model description given and the MATLAB code in Appendix A, some attention must be given to the coupling of the hydraulic step and the infiltration step. While the schemes for computing infiltration and hydraulic flow individually are well established, the coupling of the two are not widely done. If consideration is taken to the model loop nesting it is clear that having the same loop nesting for both steps would be an advantage for the coupling, giving accurate estimations of flow conditions and infiltrated length in each section, Δx. The most apparent advantage of this approach is that cumulative infiltration could be tracked separately for each section of the swale as narrow columns increasing independently for each time step the given section is wetted. While this is a good coupling method in theory, it has not been chosen as the coupling approach in this model due to its severe practical limitations. While the hydraulic equations with exemption of the initial inflow estimation, are computed only once per i and j, the implicitly solved infiltration must be iterated to convergence in each i and j using this approach. Due to the small increases in infiltration per time step as a result of the restrictions given in the hydraulic step by the Courant criteria, the iterative schemes for the cumulative

infiltration need to have a very high resolution in order to yield a difference in each step. Typically around one hundred iterations will be needed for each step in i and j, resulting in a very large amount of calculations per time step and very long model run times. This approach would make the model impossible to run practically on most computers which are readily available, especially in a the symbolic solver is implemented in the infiltration step.

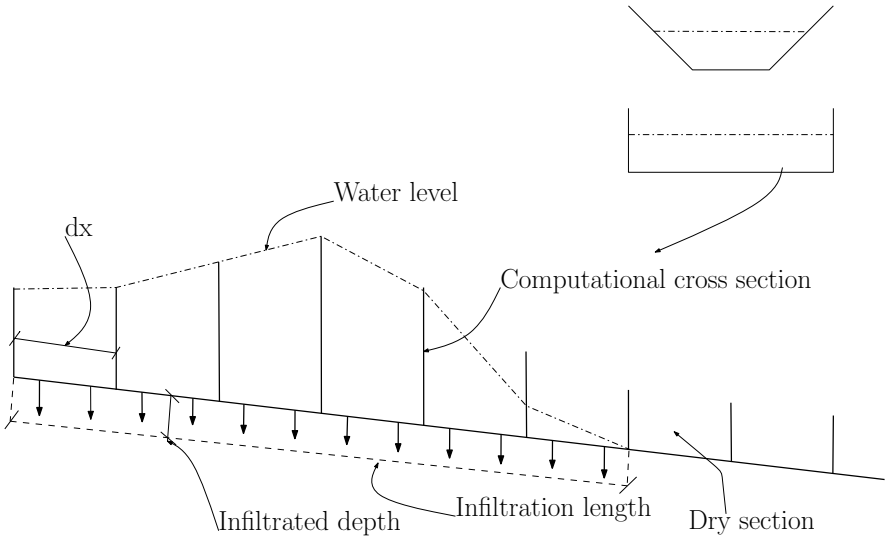

Figure 6.6: Model coupling

In order to tackle this issue a coupling has been chosen in which the cumulative infiltration is calculated only once per time step, j. Rather than controlling the spatial progress through each defined section, the wave front is tracked in order to determine the wetted length in each time step, limiting the wetted length to a maximum value equal to the swale length. There are some weaknesses in the accuracy when taking this approach which have been accepted in order to keep the model run times acceptable. Since the cumulative infiltration is presumed to progress further downward into the soil matrix for each time step and then multiplied by the wetted length and swale width, it will assume that the infiltrated depth in the added length is equal to that in the previous step. This will cause an over estimation of the infiltrated volume. In addition problems are accounted when the flood wave is falling and dry conditions have

occurred in the upstream sections of the swale, where the model does not account for dry conditions after the entire swale is wetted. This will also lead to a certain degree of over estimations of the infiltrated volume. The removed infiltrated depth from the overland flow will then consist of one small depth being removed from all depths in all i for the current time step. A graphical representation of this approach can be seen in Fig. (6.6).

The removal of the infiltrated depth will on another hand be small compared to the flow depth. This will lead to small differences in flow conditions within the current step, although large effects are expected on the swale as a whole. Due to this the infiltrated depth is removed directly from the flow without new corrections of depth and velocity through the numerical schemes described in Section 6.3. While this is a simplification in terms of removing a singe infiltrated depth from the flow depth in each step, it will bring a volumetric balance to the model. While some simplifications have been made in this step, it is expected that with proper calibration the model will yield results superior to existing methods and very close to observed field conditions.

7 Results

In this section a series of test simulations of the model described in previous sections will be conducted. While the simulations will be based on constructed data, since no field data is available for calibrating the model, key parameters will be varied in the simulations in order to make an assessment of the model limitations, strengths and weaknesses. A selection of five different simulations are to be presented, all valid for the hydrograph given in Fig. (6.5). The simulations will be based on typical swale dimensions, with a swale length of $100\,m$ and a trapezoidal cross section with a bottom width of $2\,m$ and a side slope of $4:1$. A reference simulation not including infiltration, for typical swale design parameters has also been conducted. In Table (3) input parameters for the model simulations are given, as they are denoted in the MATLAB code given in Appendix A. Note that care has been taken to standardize most simulation parameters and that changes have been made in only one parameter at the time in order to see how specific parameters will affect the simulation.

Parameter	Reference	1	2	3	4	5
length	100	100	100	100	100	100
deltax	5	5	5	5	5	5
timestep	0.1	1	1	1	1	1
numb_it	35000	3500	3500	3500	3500	3500
slope	5	5	5	5	10	5
manning	30	30	60	30	30	30
shape	2	2	2	2	2	2
B	2	2	2	2	2	2
z	4	4	4	4	4	4
soiltype	-	sand	sand	loam	sand	sand
theta_0	-	0.200	0.200	0.400	0.200	0.020
z_tot	-	100	100	100	100	100
solver	-	1	1	2	1	1

Table 3: Table of simulation parameters

7.1 Simulation Results

7.1.1 Reference Simulation

A reference simulation has been conducted in order to show how the hydraulic equations act during a completely stable simulation for a trapezoidal cross section not being influenced by infiltration. This is useful in assessing the model behavior when changes are made in time step compared to stable conditions and how the infiltration will affect the channel flow. The results are shown in Fig. (7.1) and Fig. (7.2). Note that the outflow depth is greater than the inflow depth, while the outflow velocity has been reduced accordingly. This is an indication of the channel delaying effect.

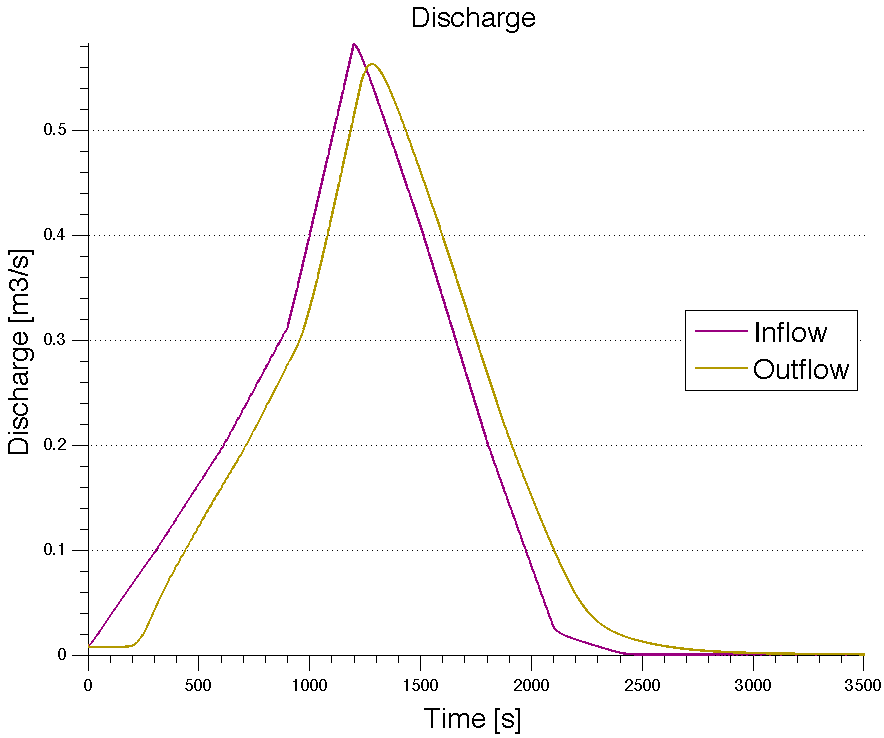

Figure 7.1: Reference simulation, Discharge

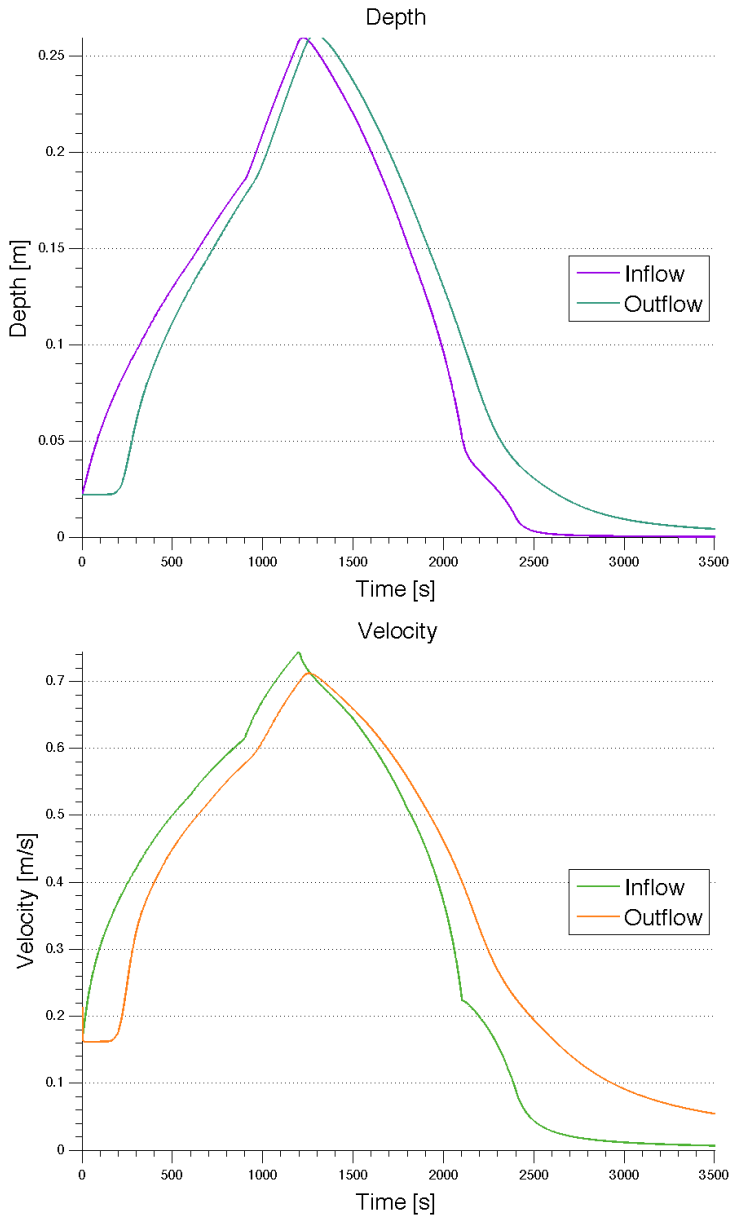

Figure 7.2: Reference simulation, Depth and Velocity

7.1.2 Simulation 1 - Standardized Swale

In simulation 1, a standardized swale has been modeled on the basis of values given by Leland (2013). Sand has been chosen as the infiltration media with moderately saturated initial conditions, as would be expected in most field cases. Saturation levels are, however, greatly dependent on meteorological and hydrological conditions at the location of the swale which is to be modeled. The results of this simulation can be seen in Fig. (7.3) and Fig. (7.4). Note a reduction of approximately $50\,l/s$ of the maximum outflow discharge and a slight retarding effect on the outflow hydrograph compared to the reference simulation. Notice should also be taken to the dip in the outflow depth and velocity at around $200\,s$ and the constant depth and velocity at the end of the simulated event.

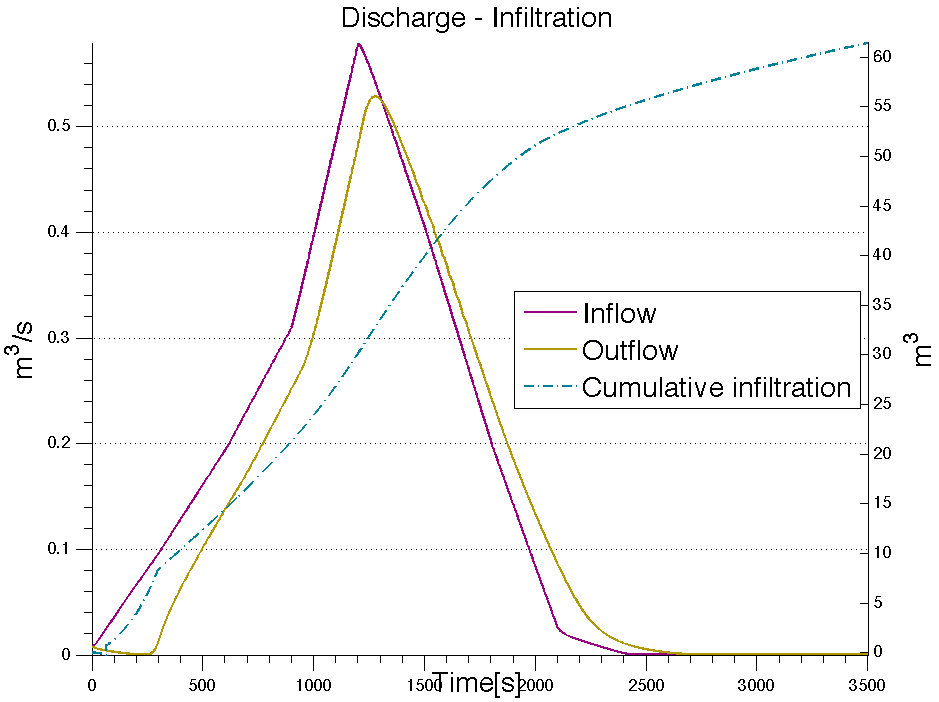

Figure 7.3: Simulation 1, Discharge - Infiltration

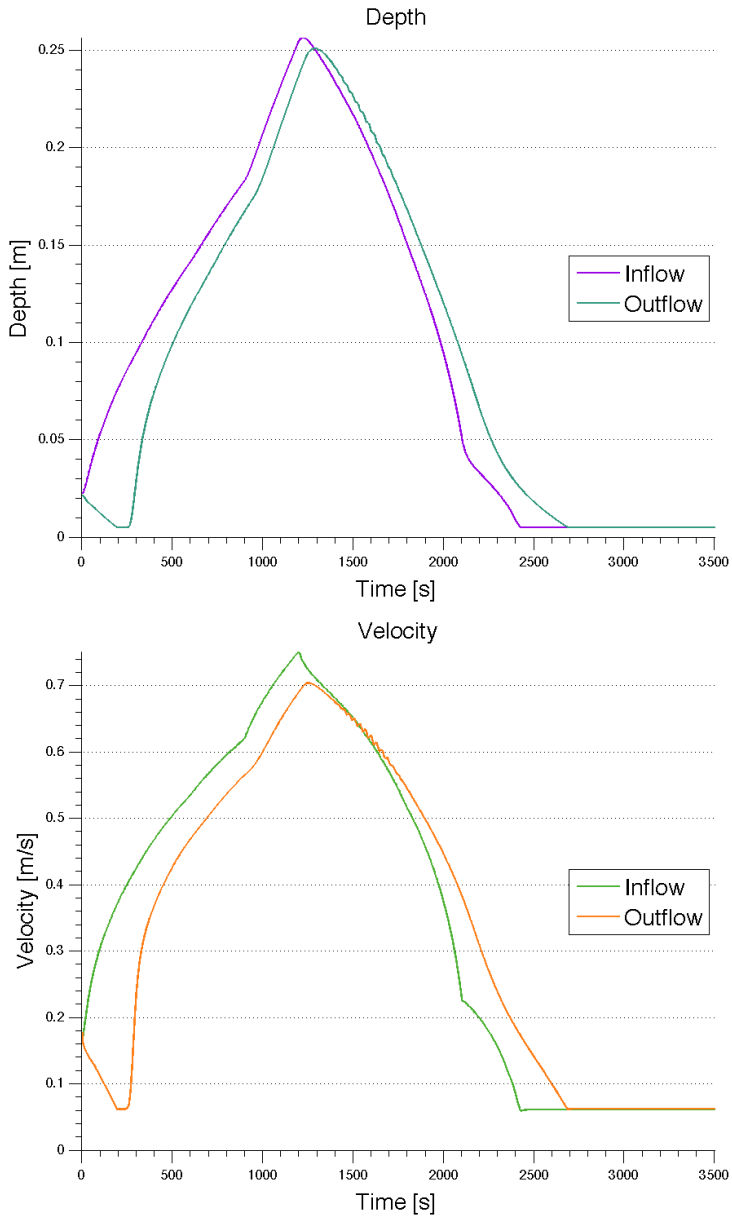

Figure 7.4: Simulation 1, Depth and Velocity

7.1.3 Simulation 2 - Increased Manning Coefficient

In simulation 2 all parameters except the Manning coefficient has been kept equal to simulation 1. While a Manning coefficient of $30\,m^{1/3}/s$ is a standardized value for flows through grass, swales can have variations brought forwards through seasonal variations or erosion. Thus making the channel smoother than usual, something which is especially true for nordic conditions in the winter season. The Manning coefficient has therefore been increased to $60\,m^{1/3}/s$, which is a fairly smooth bed surface, and results can be seen in Fig. (7.5) and Fig (7.6). Note significantly increased maximum velocity and decreased flow depth, yielding a smaller reduction of maximum outflow discharge than simulation 1. Attempts were made at lowering the Manning coefficient below $30\,m^{1/3}/s$, however the model was not able to run in these cases.

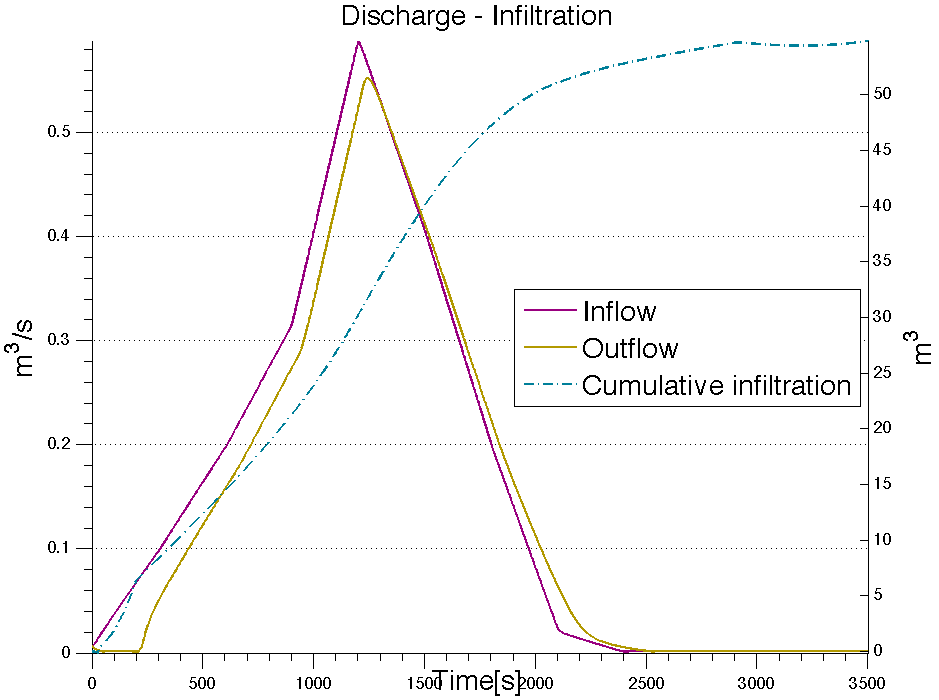

Figure 7.5: Simulation 2, Discharge - Infiltration

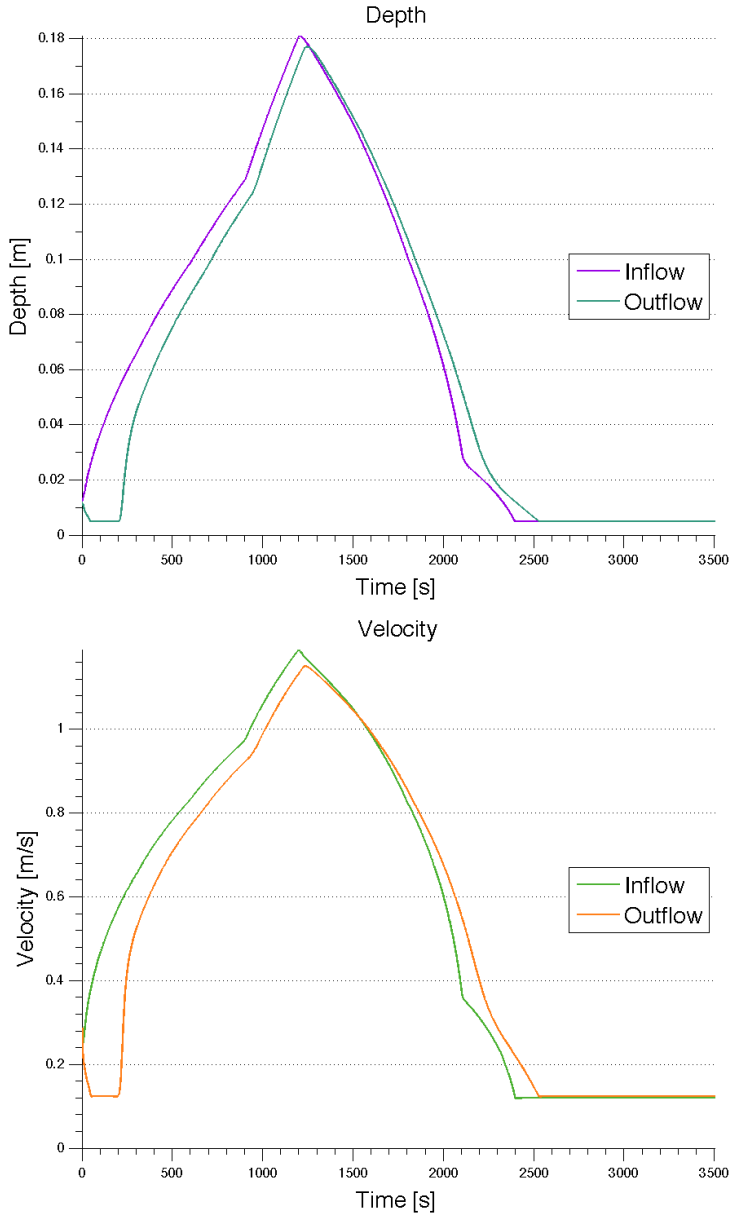

Figure 7.6: Simulation 2, Depth and Velocity

7.1.4 Simulation 3 - Nearly Saturated Loam as Infiltration Matrix

In simulation 3 the soil matrix is changed to loam with a volumetric saturation of 0.400 m^3/m^3, which is close to complete saturation. The purpose of this simulation is to investigate the models ability to simulate a range of infiltration media according to the classification system given by Rawls et al. (1982). With a fine grained and nearly saturated infiltration matrix, it is expected that very small amounts of water will be infiltrated each time step, also yielding a low total infiltrated volume. The results from simulation 3 are given in Fig. (7.7) and Fig. (7.8). Note that the solver for the infiltration in this case had to be set to the numerical solver due to the symbolic solvers inability to run stably. Also note the oscillations in the falling outflow graphs.

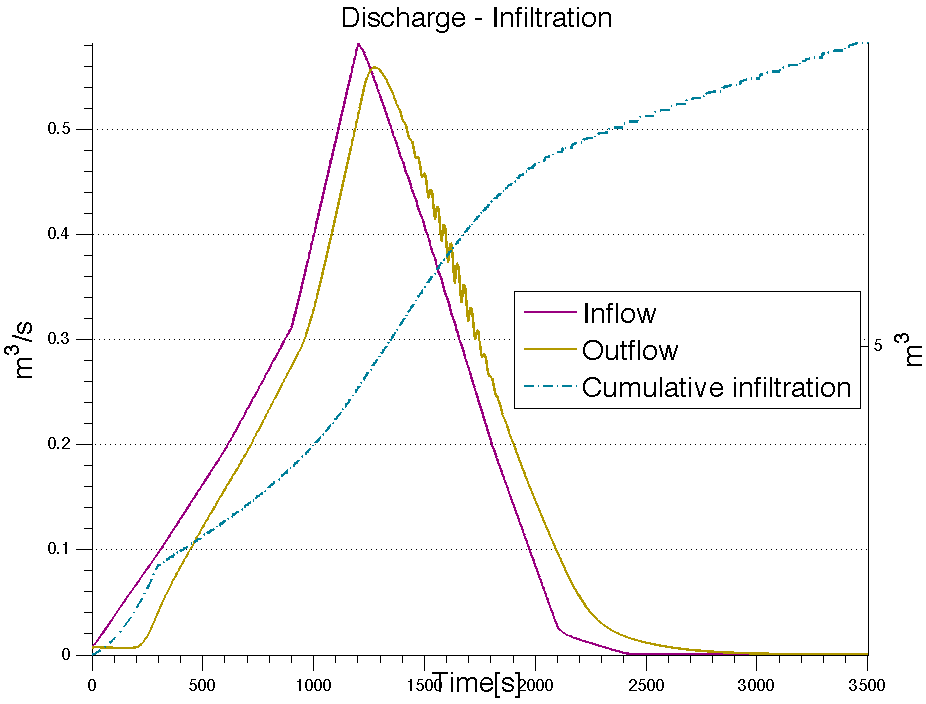

Figure 7.7: Simulation 3, Discharge - Infiltration

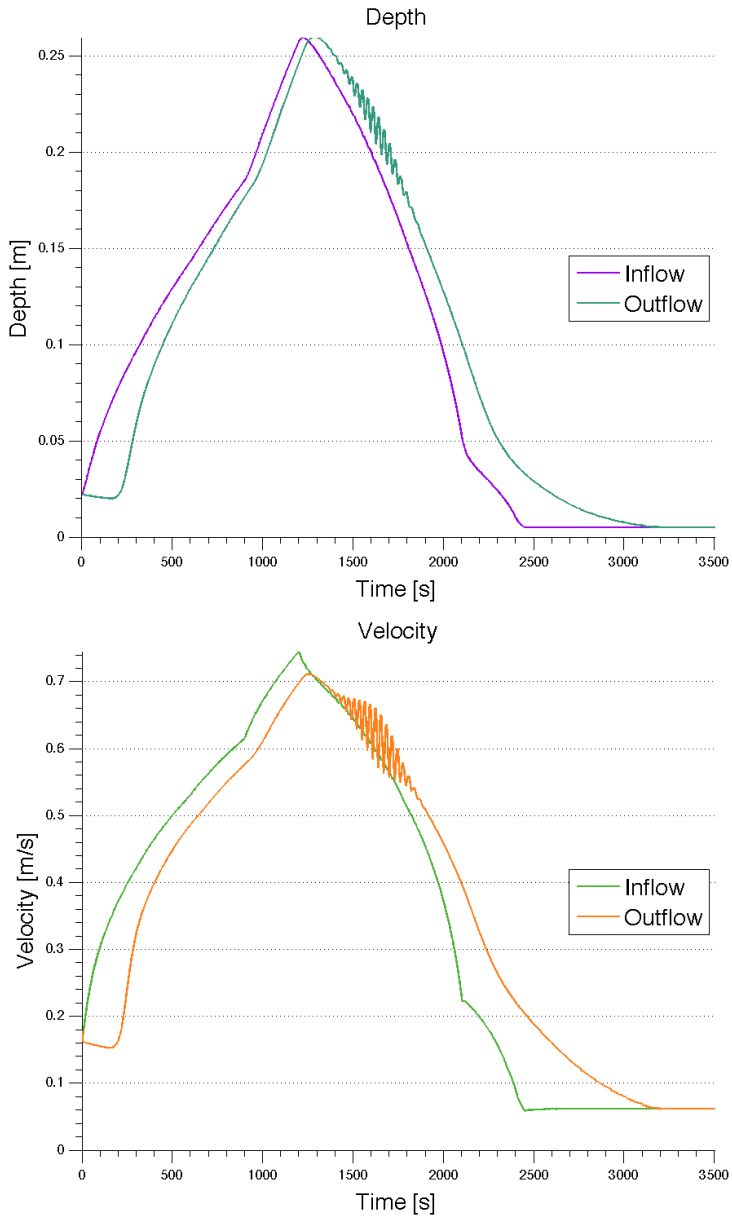

Figure 7.8: Simulation 3, Depth and Velocity

7.1.5 Simulation 4 - Increased Longitudinal Slope

Simulation 4 handles changes in the longitudinal slope. Design criteria often give a recommended maximum longitudinal slope of 5‰ in order to ensure velocities below $1m/s$, where the danger of erosion occurs. Interest may lie in investigating this further and it is important that the model is capable of modeling this. In this simulation the slope has been increased to 10‰, double the recommended slope, and the results can be seen in Fig. (7.9) and Fig. (7.10). Note the oscillations at the minimum depth in the velocity graph, indicating that a slope of 10‰ is nearing the models limitations.

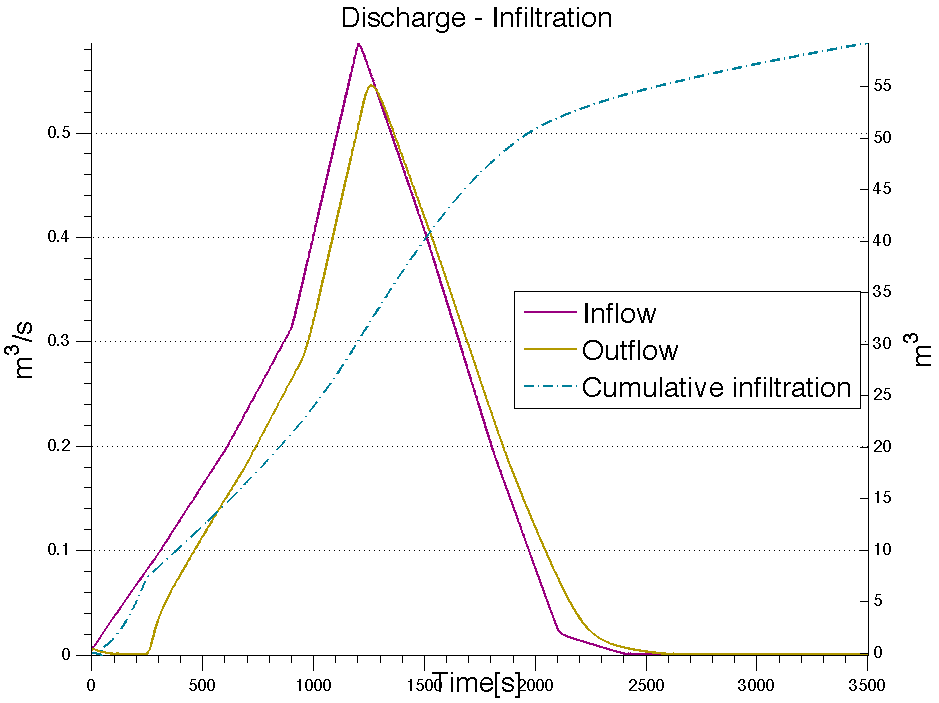

Figure 7.9: Simulation 4, Discharge - Infiltration

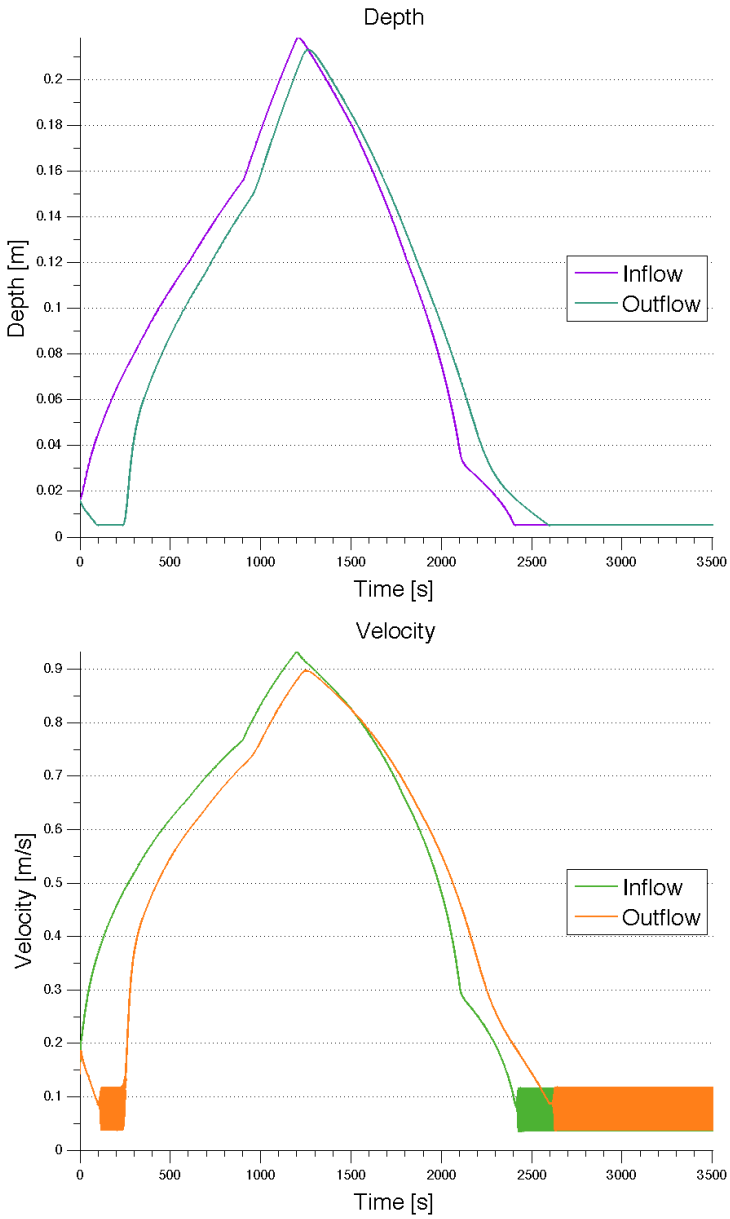

Figure 7.10: Simulation 4, Depth and Velocity

7.1.6 Simulation 5 - Completely Dry Sand

The last simulation to be presented takes into account the results of the infiltration media consisting of completely dry sand. While the infiltration media in most field conditions will be moderately saturated, the model should be able to model completely dry conditions in which the stepwise increments in infiltrated depth will be at its maximum. The combination of simulation 3 and simulation 5 will investigate the extremities of the infiltration step and the expected operational range. The results from this simulation can be seen in Fig. (7.11) and Fig. (7.12). Note the increase in total infiltrated volume as compared to simulation 1 and 3, and an even further reduction of the maximum outflow discharge.

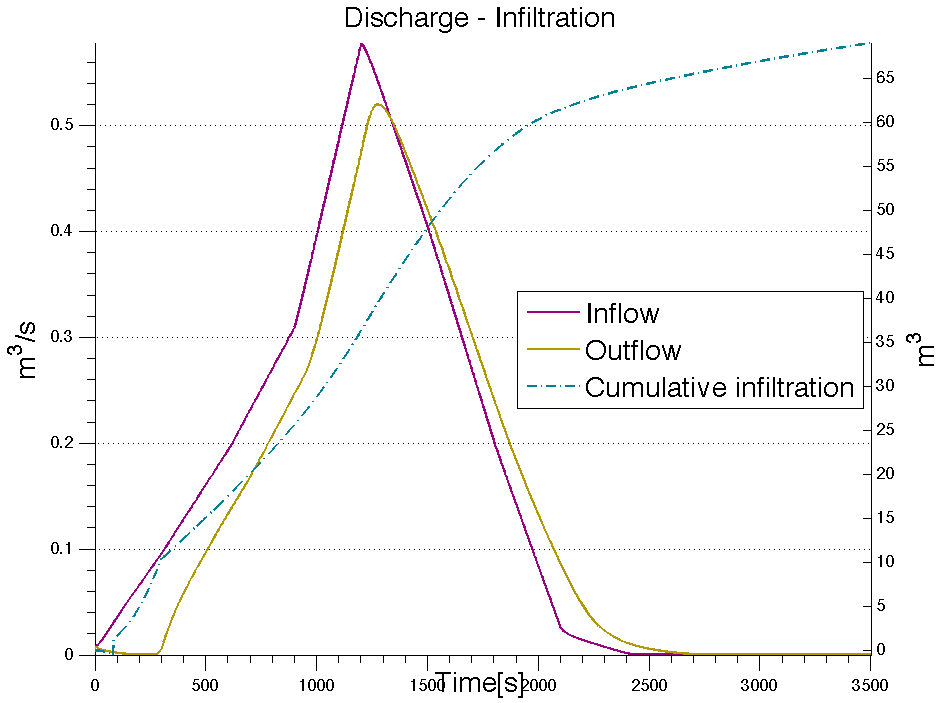

Figure 7.11: Simulation 5, Discharge - Infiltration

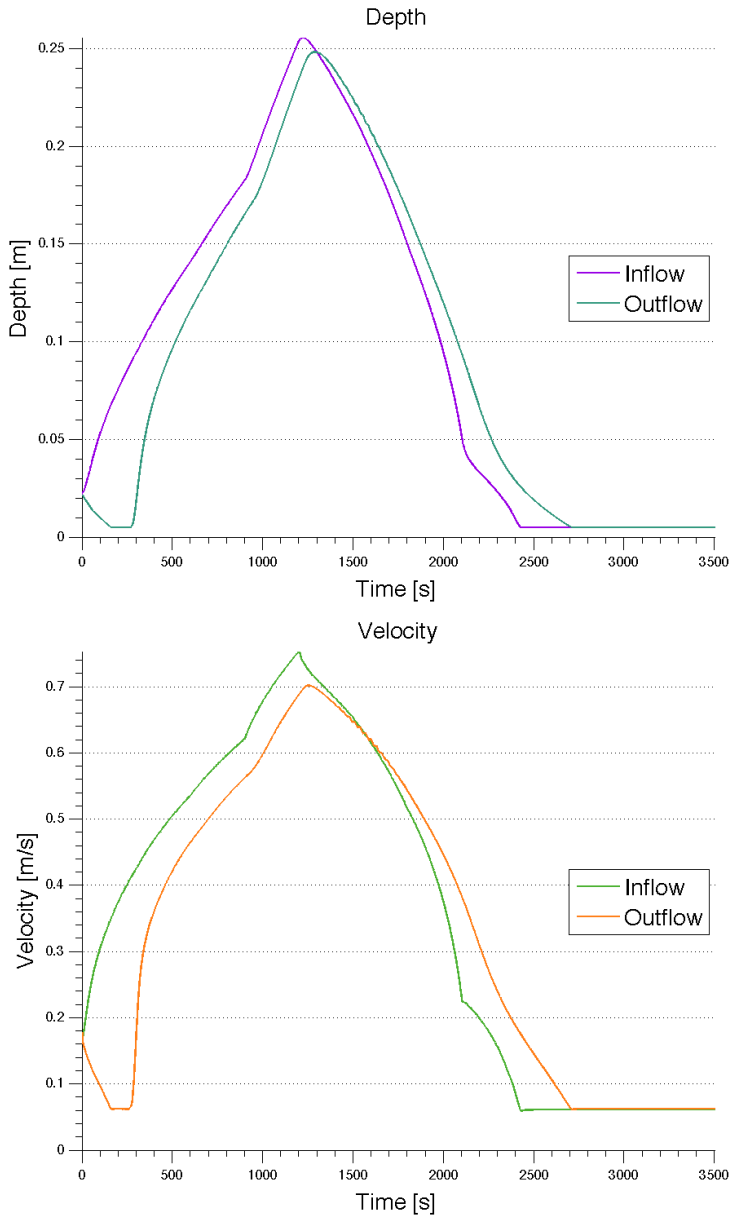

Figure 7.12: Simulation 5, Depth and Velocity

8 Discussion

When discussing the validity of the model presented in this thesis, it should ideally be done using measured field data from a specific swale for a variety of rainfall events. Such data are not available at the current time. Evaluations must therefore be done on a basis of the theoretical behavior which is to be expected from the model governing equations, and the interaction between them. In such an approach attention should be given to which parameters have the greatest impact on model stability and results, and if the model behavior is rooted within each step or if it is a result of the coupling. On a basis of the simulations in Section 7, a general recommendation can be given on what should be focused on in further work.

In general the model seems to yield results which are very close to what is expected of the theoretical basis. Some inaccuracies and simplifications are present, however the model seems to run well within the operational range indicated by the simulations. The simulations which have been run for typical swale design parameters are generally stable, and issues are encountered only when more extreme parameter values are simulated.

8.1 Hydraulic Considerations

The model hydraulic step consists of complex calculations, needing several equations and discretizations in order to be modeled properly. Therefore it is also expected that this step will be the most prone to inaccuracies and errors. There are both strengths and weaknesses within the hydraulic step which will be discussed in the following.

Perhaps the most critical consideration that must be taken in the, is a general hydraulic issue which will span multiple parameters. This is the handling of shallow depth flow, and is often regarded as a problem area within hydraulic engineering. As can be seen from all depth plots given in Section 7, large flow depths will not occur, even when the maximum discharge is quite large for an urban drainage event. At small flow depths the explicit discretization of St. Venant´s equation becomes unstable in such a way that when the water depth approaches zero, the velocity will start oscillating towards infinity. This is mainly due to the continuity equations which are combined with the St. Venant equation. These equations give the assumption that the change in volume over Δx must be balanced by the discharge, yielding conservation of mass. When the flow depth becomes very small, in this case beneath $0.005\,m$, keeping the mass continuity leads to large velocities in order to maintain the

discharge. This is especially challenging for smaller Manning coefficients where shallow flows would in reality yield very low velocities. This is to be expected in small flow conveyance in grassed swales, especially if the flow depth is around the vegetation height. In the model simulations, the instabilities due to small flow conveyance can be seen clearly in Fig. (7.10). Here a low Manning coefficient is combined with an increased longitudinal slope. While the model is capable of running stably for typical swale longitudinal slopes, increasing the slope will accentuate the oscillation issues since a larger velocity will be computed for the corresponding depth. Here it can be seen as the velocity oscillates rapidly when a certain depth is reached. In this case the oscillations are limited by a threshold depth, which will be discussed further in Section 8.3, keeping the them from increasing uncontrollably. If the depth had been allowed to continue decreasing towards zero, the oscillations would increase accordingly. In the reference simulation, Fig. (7.2), a much smaller timestep has been used, giving the ability to cope with these oscillations as according to the Courant criteria. A reduction of the time step in this order is however not possible when including the infiltration step. This is a result of the model coupling and will be discussed further in Section 8.3. In order to cope with these shallow water wetting conditions, more complex discretizations which are more robust regarding velocity calculations are often needed. Therefore thought should be given on improving the model presented in this thesis in this respect. A possible solution could be the implementation of an implicit discretization with limiting algorithms, which are set up to reduce numerical oscillations due to the continuity approach. This would, however, lead to significantly increased simulation run times as discussed previously. The practical value of making such an improvement must still be carefully evaluated. If very detailed small flow modeling is needed, which is the case if a sedimentation step is to be implemented, the added simulation detail would be beneficiary despite the added run time.

While the hydraulic step isolated is fully capable of modeling depths approaching zero given sufficiently small time steps, the model has some issues coping with the depth reaching zero at the outflow hydrograph before it is initiated. This can be seen in the reference simulation in Fig. (7.2) for $t < 300\,s$ where the outflow discharge is constant and equal to the inflow hydrograph at $t = 0$. At this point the real outflow hydrograph would have zero discharge due to the entire channel not yet being wetted. Introducing limiters setting the depth and velocity equal zero were attempted to counteract this effect, but proved unsuccessful. During these attempts, the model would not be capable of producing an outflow hydrograph, yielding a constant zero outflow throughout the entire event. This effect is most likely due to the shallow water issues as

mentioned above. The governing equations are not able to handle the wetting conditions properly, thus having the inability to lock onto the rising hydrograph when its input is given. This simplification will yield results which have larger total outflow volumes than what is observed in field conditions, and will represent a significant error for the time in which the swale is not completely wetted. When the outflow hydrograph is initiated at its given time step, the model will behave as would be expected. This issue is therefore confined to the initial stages of a swale runoff event, and will pose an error mainly due to the creation of false discharge. In addition to giving erroneous discharge volumes, it will also make it difficult conducting a proper coupling of the hydraulic and infiltration steps as the depth cannot be used as a limiting parameter. This would be the ideal way of deciding the wetted channel length. Instead a method of tracking the wave front must be used as an alternative. The simplification should be addressed when calibrating and improving the model for the same reasons as discussed in the previous paragraph.

There are also considerations to be taken on the simulation results that are bound to specific hydraulic parameters. The first parameter which should be discussed is the model behavior in respect to variations in Manning´s friction coefficient. This can be seen in simulation 1 and simulation 2 where the Manning coefficient is changed from $30\ m^{1/3}/s$ to $60\ m^{1/3}/s$. The difference between simulations 1 and 2 can be seen in that the reduction of maximum outflow discharge is smaller for $M = 60m^{1/3}/s$, that the velocity is well above $1m/s$, and the maximum depth is reduced to $0.18m$. An increase in the Manning coefficient will therefore greatly affect the flow conditions, bringing the swale flow velocity above the limit of erosion for the given event. While this is apparent for the depth and velocity, the effect on discharge is not as clear. It is important to have the ability to model a wide range of Manning coefficients such that the effects can be properly evaluated against field data. While geometrical conditions are often set in swales, the Manning coefficient must be evaluated in each case. When establishing a swale model, calibrations and verifications must be made such that the model is valid for the swale in question. The Manning coefficient is freely defined by the user, making it extremely important in this process. In swale hydraulics it is also reasonable to expect a wide range of Manning coefficients over the course of changing seasons. This is especially true for swale hydraulics in nordic climates. Here the summer seasons yield typical grassed swale flows, while in the winter seasons freezing would lead to a smoother bed roughness. In addition it might be likely that the Manning coefficient for shallow flow depths through grass is lower than the widely used value of $30\ m^{1/3}/s$, which is based on flood plain flow adjacent to large scale rivers. This subject is handled

in the research by Kirby et al. (2005), where equivalent friction coefficients for shallow depth flow through grass are given. The model presented is this thesis has a range in Manning coefficients from $30\,m^{1/3}/s$ to $60\,m^{1/3}/s$, which covers the expected practical range fairly well. Attempts were made to run simulations with Manning coefficients below $30\,m^{1/3}/s$, however these proved unsuccessful resulting in simulation failures. This is most likely due to the time step of $1\,s$ being too large, causing oscillations in the flow velocity. Attempts to reduce the time step, however, caused the infiltration step to fail. This connection will be discussed further in Section 8.3. It must also be mentioned that with the increased velocities due to a smoother channel bed, the wave front tracking becomes somewhat inaccurate. This can be seen clearly in Fig. (7.5), where the infiltration graph reaches the maximum wetted length before the outflow hydrograph is initiated. This is due to the wave front maximum channel velocity becoming too large compared to the wave front velocity. The model will track the wave front well for normal swale conditions, Fig. (7.3). Even though having a good practical range, it is desirable to improve the model allowing for larger simulation time steps by upgrading the discretization to an implicit discretization.

Another parameter which will mainly affect the hydraulic step is the channel longitudinal slope. While the longitudinal slope is taken into account also in the modified version of Green Ampt´s equation, it will be more significant in the hydraulic step. Results from increasing the slope to double the recommended slope, shows an increase in velocity combined with decreasing depths. While not as prominent as changes in the Manning coefficient, the velocity graph will show a significant increase in peak flow velocity. This is as previously mentioned especially visible when the increased velocity due to the increased slope is combined with a rough channel bed yielding oscillations. Decreasing the slope angle should not give large issues with the model stability. From the simulations it can seem that the model sensitivity to the Manning coefficient is greater than to that of the longitudinal slope. However, there could be expected some issues with uncontrolled oscillations if very low Manning´s coefficients are combined with large slopes. This is beyond the model capabilities, and reasonable swale design practice. As the simulations show, the response to the change in longitudinal slope is stable within common design criteria. This must however be confirmed through calibrations in further work.

8.2 Infiltration Considerations

Before the model can be discussed as a whole, there are some model behaviors specific to the infiltration step which must be discussed. In general, the infiltration step behaves as would be expected from the theoretical basis. From simulation 1 through 5 it is clear that the infiltration behaves in a similar way for a variety of hydraulic conditions, soil types and saturation levels. The infiltration can be seen to follow similarly shaped graphs, which could be divided into three main stages. This is shown most clearly in Fig. (7.3) where the infiltration increases exponentially up until $t \backsimeq 250\,s$, then the infiltration becomes nearly linear with a steep slope until it starts flattening out at $t = 2000\,s$. These points mark the transitions between three stages; the first stage being a partially wetted swale where the infiltration length is increasing, the second being a fully wetted swale with rapid infiltration in the top soil layer, and the third being the slowing of the infiltration flux as the soil matrix becomes more saturated. This concurs well with simulations done through Green Ampt´s equation on infiltration alone. In such a way, it is not affected to a large extent by the hydraulic step, except for the first stage. It is also clear that there is a large variation in the infiltrated volume between the simulations. As expected simulation 5 yields the largest volume at $69\,m^3$. The smallest infiltrated volume is given in simulation 3, where the volume is just below $10\,m^3$. In the remaining simulations the soil matrix is set to moderately saturated sand where a range of $55-61\,m^3$ infiltrated volume is computed, depending on the flow conditions. In general the Green Ampt equation seems to compute correctly within the model as a whole.

There are still some model behaviors that can be connected mainly to the infiltration equation. The first of which is the behavior of the infiltration step for $t < 60\,s$, which can be seen in Fig. (8.1(a)). The infiltration starts of at zero before decreasing negatively until suddenly stabilizing for positive values at $t > 60\,s$, following the expected behavior from there on. While the graph shown in Fig. (8.1(a)) is based on simulation 1, the same is true for all other simulations implementing the symbolic infiltration solver. The reason for this behavior is most likely the time step chosen for the simulations being too small. As given in Section 5.2, Green Ampt´s equation is intended for modeling infiltration in (cm) and (h), while the model developed in this thesis is based on time steps given in (s), which presents a significant difference. This erroneous behavior is therefore most likely a result of the symbolic solver converging on an imaginary negative value of I, which is closer than the real positive value of I for these time steps. This also explains the sudden leap in infiltration which occurs at $t = 60\,s$,

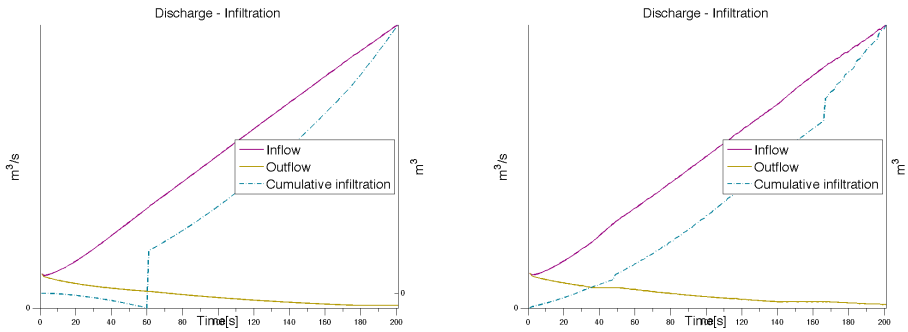

(a) Symbolic solver (b) Numerical solver

Figure 8.1: Detail, Simulation 1, discharge - infiltration, excerpt from Fig. (7.3)

where the positive value of convergence becomes nearest for the current time step. For time steps above this point the infiltration curve is smooth, which is a clear sign of high accuracy. While this is true for the symbolic solver, a duplicate simulation has been conducted implementing the option of using the numerical solver for Green Ampt´s equation. All other parameters are kept the same, and the excerpt is shown in Fig. (8.1(b)). Here it is apparent that the same issue is not present in the numerical solver in the way that the infiltrated volume is steadily increasing. The reason behind this is that the symbolic solver uses an algorithm which jumps back and forth variably until the nearest value for convergence is reached. The numerical solver, however, is set to initiate at the value of the previous infiltrated depth and increase in constant positive steps. As a result the numerical solver is unable to produce negative values and therefore converges solely on the positive value of convergence. However, if regard is taken to the remaining curve it is clear that the curve is much more uneven for the numerical solver than for the symbolic solver, indicating more inaccurate iterations. When making a choice between the two solvers, it must also be remembered that the initial 60 seconds of the simulation results in a very small amount of the total infiltration. Thus making this error fairly negligible for the simulation in its entirety. Fig (8.1) does however shed light on certain properties in the two different solvers; while the symbolic solver yields the highest accuracy apart from the initial 60 s, the numerical solver grants greater stability at the cost of total accuracy.

The second behavior that must be discussed regarding the infiltration step, is the models reaction to changes in soil type from porous sand to more fine grained soil types such as loam and silt. As can be seen in Table (3), all simulations are run implementing the symbolic solver except for simulation 3 where nearly saturated loam has been modeled. In this simulation the numerical solver had to be implemented due to the model being unable to run for fine grained soil types while implementing the symbolic solver. It can also be seen that the infiltration graph in Fig. (7.7) is more uneven than the other simulations, especially for $t > 2000\ s$ where the infiltration enters the third stage. The general shape of the graph and behavior of the infiltration equation is otherwise as expected. The reason why the symbolic solver is unable to model these conditions is most likely due to a much more rigorous iteration accuracy demand. When small time steps are combined with fine grained soil types the change in infiltrated depth in each time step will be very small, leading to convergence issues. In such a way the small increments will not be able to converge within the symbolic threshold accuracy. While this poses a problem for the symbolic solver, the numerical solver has much lower demands for reaching convergence. It is therefore able to overcome the issues with very small increments in infiltration. This fact will therefore further confirm that while being slightly more inaccurate, the numerical solver is a more robust solver than the symbolic.

8.3 Coupling Considerations

While some of the model behaviors can be linked mainly to one of the computational steps, the most significant issues are results of the coupling of the two. Perhaps the most prominent effect of the coupling is the effect and limitations given in the time step parameter. The explicit discretizations of St. Venant´s equation require very small time steps in order to cope with flow depths approaching zero. Green Ampt´s equation and its solvers become more unstable the smaller time step is used. In the model established in this thesis, the main loop in which both steps are nested is governed by the time step. This therefore makes it necessary calculating both infiltration and flow depth and velocity every time step. Therefore a very strict limitation is given in the choice of time step, where a time step of $1\ s$ has been found to run combined simulations with acceptable accuracy and stability. Choosing smaller time steps will lead to the infiltration step not being able to converge, and choosing larger time steps will result in oscillations as can be seen in Fig. (7.10). In order to stabilize this strict time step range, an artificial threshold depth equal to $0.005\ m$ has been introduced. It is activated as a limiter when the infiltration step is included

in the simulation. The same has not been done for simulations where the infiltration step is not included, due to the possibility of reducing the time step further in order to ensure stability. This can be seen in the reference simulation in Fig. (7.1) and Fig. (7.2). In Fig. (7.3) through Fig. (7.12) the effect of the introduction of the threshold depth can be clearly seen in the depth and velocity plots. Here the outflow graphs are limited to constant values. While this is a simplification which prevents properly modeling the wetting - drying behavior, it is necessary to include in order to achieve model stability. While this will give a threshold for ponded conditions and therefore wetting and drying of the swale channel bed, it will not be able to recreate the detailed physical behavior of the wetting and drying process. In addition the introduction of an artificial threshold depth will in reality introduce an increased water volume which is not a result of the inflow hydrograph, and therefore create a source of errors. A possible solution to this issue would be to improve the hydraulic step with implicit or semi implicit discretizations, allowing the model to run stably for larger time steps. This would be a more reasonable approach than attempting to modify the Green Ampt equation further because of its intended use on time steps in the range of hours. Yet, it must be commented that while apparent in the depth and velocity plots, these errors will not translate significantly to the discharge.

While the severe limitations in choice of time steps might be the most important issue resulting from the model coupling, another coupling issue can be seen in Fig. (7.7) and Fig. (7.8). Here the the numerical solver is implemented in the infiltration step, and additional inaccuracies to the ones discussed in Section 8.2 can be seen. It is clear that the infiltration step causes instabilities and errors at the falling hydrograph which coincides with the transition from the second to the third infiltration stage at the time range $t = [1500 : 2000]s$. These oscillations are shown most clearly in the velocity plots, but will also translate significantly to the discharge and depth plots. The reason behind this behavior is most likely inaccurate convergence in the numerical infiltration solver as discussed previously. As stated, the coupling of the steps consists of a single infiltrated depth being removed from the flow depth in each time step. The combination of unstable iterations and fluctuating infiltrated depths, combined with the falling hydrograph will lead to the combined model having difficulties in stabilizing adequately. While it could be expected that this would be an issue for the entire event, it is only seen at the falling hydrograph. This is because St. Venant´s equation is more prone to instabilities in falling wave conditions. The same effect can also be seen in simulation 1 and 5 although it is much less prominent due to the symbolic solver being implemented. This is further backed

by unsuccessful simulations which have been run with too large time steps. Here the model has failed by the velocity approaching infinity in the same time range. While these errors do not affect the infiltration, and the impact on discharge is within acceptable ranges, the depth and especially velocity implications could be of importance if the model is to expanded in order to take into account a sedimentation step. In order to improve upon the model, the limiting equation is the fairly unstable St. Venant´s equation which makes an implicit discretization a possibility. This will allow for stability for greater time steps, and thus also improving the accuracy of the Green Ampt solvers as discussed previously.

In addition to the time step based model behaviors, another aspect of the coupling must be discussed. This is the coupling method of the two steps itself, which is mentioned briefly in Section 6.6. The coupling consists of tracking the wave front and increasing the wetted length up until the total swale length is reached. This is done by tracking the swale maximum velocity in each time step and adding a small length to the wetted length. While being a fairly efficient way of establishing an accurate wetted length, this method does not take into account drying conditions. It will therefore not reduce the wetted length, resulting in an over estimation of the infiltrated volume when the runoff event is nearing its end.

Some errors in estimating the infiltrated volume will also occur at the first infiltration stage, where the wetted length is gradually increasing. A graphical representation of this can be seen in Fig. (8.2) picturing longitudinal and lateral cross sections of a swale.

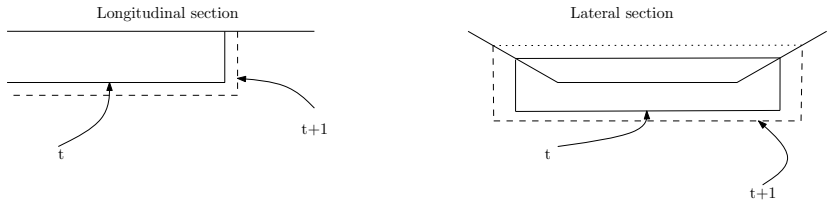

Figure 8.2: Wetting stage infiltration simplification

Here it can be seen that when the time increases from t to $t+1$, the infiltration length is increased a small amount. At the same time the infiltration depth is increased according to the infiltration step. The infiltrated depth in the added length is then set to have a cumulative infiltrated depth equal to the remaining wetted length. In reality this added length would have zero previous infiltration, and as the wetted length increases a gradual wetting front would be expected.

The same is true if the lateral cross sections are taken into account, due to the trapezoidal shape. The swale width used in order to calculate infiltrated volume from infiltrated depth is set equal to the channel top flow width, and will also over estimate the infiltrated volume in a similar way. While these errors are apparent in the first infiltration stage, they become less significant as the entire swale length becomes wetted due to the first stage yielding a small part of the total infiltrated volume.

There are also other limitations resulting from this coupling. While the depth is computed for all spatial steps in each time step, the infiltration is only computed once in each time step. Both in presenting flow depth input in Green Ampt´s equation and in removing the infiltrated depth from the flow depth, simplifications needed to be made in order to achieve manageable model run times. In this model the flow depth in Green Ampt´s equation is set to the average flow depth along the wetted length. The corresponding mean infiltrated depth is removed from the flow depth in each spatial step. This will also account for a certain over estimation of the infiltrated volume for a runoff event.

It is, however, important reviewing these simplifications and their importance in the model as a whole up against the governing equations. It should also be noted that these simplifications are results of the model build up and not the solvers or discretization methods. As presented in Section 5.2, Green Ampt´s equation will compute infiltration only in the direction normal to the swale bed slope. As the infiltration media in field observations also will experience lateral and longitudinal fluxes, it is reasonable to expect that the Green Ampt equation itself will under estimate the infiltrated depth. The over estimation due to the coupling in the model established in this thesis might therefore to a certain degree counteract this weakness within the Green Ampt equation. While the coupling therefore might seem to be heavily simplified from a mathematical view, the same might not be the case when comparing the results to field data. Regarding improvements on the model in this respect, it should be calibrated against field data, which are not available at the time this thesis is written, before conclusions can be made on its validity.

While much of the previous discussion is focused on the model errors and the causing factors, it should still be noted that the model in general responds very well according to what is expected from the governing equations. As the infiltration graphs act as would be expected, there is also a clear reduction in outflow discharge when the simulations are compared to the reference simulations in Fig. (7.1). Here a reduction in outflow discharge from $0.6\,m^3/s$ to $0.57\,m^3/s$ can be observed. In simulation 1 through 5 the peak outflow is in the range of $0.52 - 0.56\,m^3/s$ given the same initial peak discharge as the ref-

erence simulation. These results are clear indications that the use of swales will significantly reduce flooding events. While these reductions might not seem large, it must be remembered that the simulated swale is fairly short at a length of 100 m, and that the reduction of peak outflow will be much clearer as the swale length increases. This can therefore be seen as a certain confirmation of the abilities of swales within the reduction of flooding events. It is expected that the model will give an accurate mathematical and physical representation of combined swale hydraulics and infiltration, given the proper calibration and validation based on suitable field measurement data. If, however, the model is to be expanded to also take into account sedimentation and water quality parameters, improvements should be considered in order to cope with the above mentioned issues within wetting and drying combined with the time step range.

In order to sum up the simulations and discussion regarding the model behavior presented in this section, some comments must be made. During the simulations a single parameter was varied between each simulation in order to assess how the model would behave compared to a reference simulation. While this in its essence consists of a basic sensitivity analysis, where the soil type and Manning coefficient can be identified as the most sensitive parameters, strong conclusions cannot be made on the basis of the these assumptions. Although some general expectations can be drawn, a full sensitivity analysis would require the use of field data in a calibrated and validated model. In this thesis such an approach has not been possible, and the results should be interpreted as such. Expanding on the analysis using constructed data would be very prone to errors in the way that there are still many uncertainties that might be undiscovered, affecting the results. Such an analysis should be conducted when calibration data are made available, giving the scope for further work within swale hydraulics.

9 Concluding Remarks

In this thesis a semi empirical, semi explicit numerical model capable of modeling combined swale hydraulics and infiltration has been established and evaluated on a basis of constructed data. The model is capable of modeling both infiltration and overland flow in a way that concurs well with the expected behavior of the governing equations, St. Venant´s equation and Green Ampt´s equation. A clear reduction of the peak outflow discharge during a runoff event is observed. There are, however, two key issues that should be looked into in further work. The first being the limitations in time step range due to the different operating limits of the two computational steps, and the resulting need of an artificial threshold water depth. The second being the model coupling. A recommended procedure in order to handle these issues would be to implement an implicit discretization in the hydraulic step allowing for the use of larger time steps. Considerations should be made to also compute the infiltration in each spatial step. The need for addressing these issues will however depend on the models intended usage. If the model is to be expanded to include a sedimentation and water quality step, these issues should be looked into due to the need for detailed shallow flow modeling. This will, however, greatly increase the computational power needed. If the model is to be used in order to assess the hydraulic behavior of swales, as is the scope of this thesis, the current model is expected to yield results which will concur well with field conditions given the needed calibration and verification. In order to perform this, further data is needed and field measurements must be conducted, where swale inflow, outflow and soil matrix saturation must be measured. The model must then be calibrated in order to replicate the observed data for several independent runoff events. In order to fully assess the model behavior, this process must be conducted as further work beyond the scope of this thesis, while taking into account the recommendations hereby given.

Regardless of the models use within water quality assessment or hydraulic flooding response, it is clear that the established model takes into account factors beyond existing methods of swale modeling within urban drainage. As the use of swales becomes more wide spread, it is clear that the need for understanding how such solutions work in detail is increasing. While the model presented in this thesis is a step in this direction, further research is needed within the urban drainage hydraulics. In such a way a bridge between hydrology and hydraulics must be built, and strengthened, in order to create a solid foundation for further developments.

References

Bäckström, M.: 2002, *Grassed Swales for Urban Storm Drainage*, Doctoral thesis, LuleåUniversity of Technology.

Bouchard, N. R., Osmond, D. L., Winston, R. J. and Hunt, W. F.: 2013, The capacity of roadside vegetated filter strips and swales to sequester carbon, *Ecological Engineering* **54**, 227–232.
URL: *http://linkinghub.elsevier.com/retrieve/pii/S0925857413000335*

Chen, L. and Young, M. H.: 2006, Green-Ampt infiltration model for sloping surfaces, *Water Resources Research* **42**(7), n/a–n/a.
URL: *http://doi.wiley.com/10.1029/2005WR004468*

Davis, A. P., Stagge, J. H., Jamil, E. and Kim, H.: 2012, Hydraulic performance of grass swales for managing highway runoff., *Water research* **46**(20), 6775–86.
URL: *http://www.ncbi.nlm.nih.gov/pubmed/22099481*

Deletic, A.: 2001, Modelling of water and sediment transport over grassed areas, *Journal of Hydrology* **248**, 168–182.
URL: *http://www.sciencedirect.com/science/article/pii/S0022169401004036*

Dingman, S. L.: 2008, *Physical Hydrology*, 2nd edn, Waveland Press, Inc., Long Grove, Illinois.

Gilliam, J., Parsons, J. E. and Muñoz Carpena, R.: 1999, Modeling hydrology and sediment transport in vegetative filter strips, *Journal of Hydrology* **214**(1-4), 111–129.

Grinden, A.: 2013, *Hydraulic Impact of Swales in Urban Environments*, Project thesis, Norwegian University of Science and Technology.

Hood, A., Chopra, M. and Wanielista, M.: 2013, Assessment of Biosorption Activated Media Under Roadside Swales for the Removal of Phosphorus from Stormwater, *Water* **5**(1), 53–66.
URL: *http://www.mdpi.com/2073-4441/5/1/53/*

Kirby, J. T., Durrans, S. R., Johnson, P. D. and Pitt, R.: 2005, Hydraulic Resistance in Grass Swales Designed for Small Flow Conveyance, *Journal of Hydraulic Engineering* **131**(1), 65–68.

Lantin, A. and Member, A.: 2005, Design and Pollutant Reduction of Vegetated Strips and Swales.

Leland, T.: 2013, *Gresskledde vannveger i norsk klima*, Masters thesis, Norwegian University of Science and Technology.

Lindholm, O., Endresen, S., Thorolfsson, S., Sæ grov, S., Jakobsen, G. and Aaby, L.: 2008, R162 - Veiledning i klimatilpasset overvannshåndtering, *Technical report*, Norsk Vann, Hamar.

Muthanna, T. M., Viklander, M., Blecken, G. and Thorolfsson, S. T.: 2007, Snowmelt pollutant removal in bioretention areas., *Water Research* **41**(18), 4061–4072.

Naot, D., Nezu, I. and Nakegawa, H.: 1996, Hydrodynamic Behaviors of Partly Vegetated Open Channels, *Journal of Hydraulic Engineering* **122**(NOVEMBER), 625–633.

Olsen, N. R. B.: 2011, *Modelling and Hydraulics*, number January, 3rd edn, The Norwegian University of Science and Technology, Trondheim.

Pitt, R., Nara, Y., Kirby, J. and Durrans, S. R.: 2008, Particulate Transport in Grass Swales, *Low Impact Development* pp. 191–204.
URL: *http://ascelibrary.org/doi/abs/10.1061/41007%28331%2917*

Rawls, W. J., Brakensiek, D. L. and Saxton, K. E.: 1982, Estimation of Soil Water Properties, *Transactions of the ASAE* **25**(5), 1316–1320 & 1328.

Salvucci, G. D. and Enthekhabi, D.: 1994, No Title, *Water Resources Research* **30**, 2661–2661.

Schueler, T. R.: 1987, Controling urban runoff: A practical manual for planning and designing urban BMPs, *Technical report*, Washington Metropolitan Water Resources Planning Board, Washington, DC, USA.

Stagge, J. H., Davis, A. P., Jamil, E. and Kim, H.: 2012, Performance of grass swales for improving water quality from highway runoff., *Water research* **46**(20), 6731–42.
URL: *http://www.ncbi.nlm.nih.gov/pubmed/22463860*

Stahre, P.: 2006, *Sustainability in urban storm drainage - planning and examples*, 1st edn, Svensk Vatten, Malmö.

A MATLAB code

```
% Explicit solution of St. Venant equations combined with implicit solution
% of Green Ampts infiltration equation. Will compute one dimensional swale
% flow for rectangular and trapezoidal cross sections.
%
% Source St. Venant:
% Numerical Modelling and Hydraulics, 3rd edition, 9. March 2013
% http://folk.ntnu.no/nilsol/tvm4155/flures6.pdf

clear all % fresh start
close all % no open windows

format long

%%%%%%%%%%%%%%%%%%%%%%%% Input Channel Geometry%%%%%%%%%%%%%%%%%%%%%%%%%

prompt = 'Length of channel [m] = ';
length = input(prompt);

prompt = 'Lengthwise step [m] = ';
deltax = input(prompt);

prompt = 'Timestep [s] = ';
timestep = input(prompt);

prompt = 'Number of iterations = ';
%Plotting time = number of it. * timestep
numb_it = input(prompt)+1;

prompt = 'Channel lengthwise slope [x/1000] = ';
slope = input(prompt)/1000;

prompt = 'Mannings number [M] = ';
manning = input(prompt);

prompt = ['Swale cross section shape \n'...
    '[1 = rectangular, 2 = trapezoidal] = '];
shape = input(prompt);
```

```
if shape == 1;

    prompt = 'Bottom width of channel [m] = ';
    B = input(prompt);

elseif shape == 2;

    prompt = 'Bottom width of channel [m] = ';
    B = input(prompt);

    prompt = 'Side slope [x:1] = ';         %Side slope angle
    z = input(prompt);

end

%%%%%%%%%%%%%%%%%%%%%%%%%%%%Soil charactheristics %%%%%%%%%%%%%%%%%%%%%%%%%%%

prompt = 'Include infiltration step [Y=1/N=0] ?';
infiltration_step = input(prompt);

if infiltration_step == 1

prompt = ['Define soil characteristics from list \n \n \n sand = 1'...
    '\n loamy_sand = 2 \n sandy_loam = 3 \n loam = 4 \n silt_loam = 5'...
    '\n sandy_clay_loam = 6 \n \n = '];
soiltype = input(prompt);

%%%From Rawls et al 1982 "Estimation of soil water properties"%%%%%

if soiltype == 1

    K_sat = 21.00;              %Saturated hydraulic conductivity [cm/h]
    theta_sat = 0.437;          %Max volumetric saturation [cm^3/cm^3]
    psi = 7.26;                 %Suction pressure head [cm]

    prompt = 'Initial soil saturation (0.020-0.437 [cm^3/cm^3]) = ';
    theta_0 = input(prompt);
```

```
elseif soiltype == 2

    K_sat = 6.11;
    theta_sat = 0.437;
    psi = 8.69;

    prompt = 'Initial soil saturation (0.035-0.437 [cm^3/cm^3]) = ';
    theta_0 = input(prompt);

elseif soiltype == 3

    K_sat = 2.59;
    theta_sat = 0.453;
    psi = 14.66;

    prompt = 'Initial soil saturation (0.041-0.453 [cm^3/cm^3]) = ';
    theta_0 = input(prompt);

elseif soiltype == 4

    K_sat = 1.32;
    theta_sat = 0.463;
    psi = 11.15;

    prompt = 'Initial soil saturation (0.027-0.463 [cm^3/cm^3]) = ';
    theta_0 = input(prompt);

elseif soiltype == 5

    K_sat = 0.68;
    theta_sat = 0.501;
    psi = 20.76;

    prompt = 'Initial soil saturation (0.015-0.501 [cm^3/cm^3]) = ';
    theta_0 = input(prompt);

elseif soiltype == 6

    K_sat = 0.43;
```

```
    theta_sat = 0.398;
    psi = 28.08;

    prompt = 'Initial soil saturation (0.068-0.598 [m^3/m^3]) = ';
    theta_0 = input(prompt);

end

prompt = 'Drainage layer thickness [cm] = ';
z_tot = input(prompt);

prompt = 'Infiltration step solver. [1 = symbolic, 2 = numerical] = ';
solver = input(prompt);

gamma = atan(slope);                    % Longitudinal slope in degrees

end

%%%%%%%%%%%%%%%%%%%%%%%%%%%%%%%%%%%%%%%%%%%%%%%%%%%%%%%%%%%%%%%%%%%%%%%%%%%%%%%


sections = (length/deltax)+400;         %Added 400 for plot extension

disp('Working...')

% Reading time series from input hydrograph

in = load('inflow.txt');
out_q = fopen('outflow.txt','w');           % Clean output files
fclose(out_q);
out_y = fopen('depth.txt','w');
fclose(out_y);
out_u = fopen('velocity.txt','w');
fclose(out_u);
out_inf = fopen('infiltration.txt','w');
fclose(out_inf);

timein = in(:,1);
qinn = in(:,2);
```

```
n = size(in,1);
m_temp = max(in,[],1);
m = max(m_temp);
tol_depth = 0.005;       %Dry cell limit, 5mm


%%%%%%%%%%%%%%%%%%%%%%%%%%%% Initialization %%%%%%%%%%%%%%%%%%%%%%%%%%%%%%%%

%%%%%%%%%%%%%%%%%%%%%%% 1. Determine inflow u and y %%%%%%%%%%%%%%%%%%%%%%%%

%%%%%%%%%%%%%%%% Iteration loop rectangualar channel %%%%%%%%%%%%%%%%%%%%%%%

if shape == 1,

    y_old = zeros(1,200);
    y_new = zeros(1,200);

        for i = 2:200

        y_old(1) = 1;

        y_new(i-1) = qinn(1)/(manning*B*((B)/((B/y_old(i-1))+2))^(2/3)...
            *sqrt(slope));

        y_old(i) = y_new(i-1);

            if (abs(y_old(i)-y_old(i-1))) < 0.0001

                y = y_old(i);

                if y < tol_depth

                    y = tol_depth;

                end

                break

            end
```

```
        end

    A = B*y;
    u = qinn(1)/A;
    R = A/(2*y+B);


%%%%%%%%%%%%%%%%%% Iteration loop trapezoidal channel %%%%%%%%%%%%%%%%%%%%


elseif shape == 2,


    control_iter = zeros(1,1000);
    y_iter = zeros(1,1000);

    for i = 2:5000

                control = qinn(1)/(manning*sqrt(slope));

                y_iter(1) = 0;

                control_iter(i) = (B*y_iter(i-1)+z*(y_iter(i-1))^2)*...
                    ((B*y_iter(i-1)+z*(y_iter(i-1))^2)/...
                    (sqrt(B+z*y_iter(i-1)*(1+z^2))))^(2/3);

                if (abs(control-control_iter(i))) < 0.001

                    y = y_iter(i-1);

                        if y < tol_depth;       %Dry cell limitation

                            y = tol_depth;

                        end

                    break
```

```
                end

                y_iter(i) = y_iter(i-1)+0.001;  %Threshold accuracy 1mm

    end

    B_top = B+2*z*y;
    A = ((B+B_top)/(2))*y;
    u = qinn(1)/A;
    R = A/(B+2*sqrt(y^2+(z*y)^2));

end

depth(1:sections+1,1:2) = y;        %Vector preparation for St. Venants
velocity(1:sections+1,1:2) = u;

if shape == 1

    area_rect(1:sections+1,1:2) = A;
    R_hyd(1:sections+1,1:2) = R;

elseif shape == 2                   %Trapezoid area for discretization

    area_trap(1:sections+1,1:2) = A;
    B_t(1:sections+1,1:2) = B_top;
    R_hyd(1:sections+1,1:2) = R;

end

%%%%%%%%%%%%%%%%%%% Initialize infiltration step %%%%%%%%%%%%%%%%%%%%%%%%%

if infiltration_step == 1           %Calculates infiltration depth in cm

    I = zeros(numb_it,1);           %Starting with no infiltration i,1
    I_diff = zeros(numb_it,1);
    I_vol = zeros(numb_it,1);
    inf_control = zeros(3000,1);
    inf_control_0 = zeros(3000,1);
```

```
iter_inf_0 = zeros(3000,1);

inf_length = u*timestep;        %Initialize wetted length
I_tot_vol = zeros(numb_it,1);

if y > tol_depth

    if solver == 1      %Implements MATLAB integrated symbolic solver.

        syms I_solver_0

        old = digits;

        digits(10);             %Solver accuracy

        I_0 = vpasolve(K_sat*(timestep/(60*60))*cos(gamma)...
            +((psi+y*100*cos(gamma))*(theta_sat-theta_0))...
            /(cos(gamma))*log(1+(I_solver_0*cos(gamma)/...
            ((psi+y*cos(gamma))*(theta_sat-theta_0))))==I_solver_0,...
            I_solver_0, K_sat*(timestep/(60*60))*cos(gamma));

        double(I_0);

        digits(old);

    elseif solver == 2          %Numerical solver based on iterations

    for l = 2:3000

    inf_control_0(1) = K_sat*(timestep/(60*60))*cos(gamma);

    inf = K_sat*(timestep/(60*60))*cos(gamma)...
        +((psi+y*100*cos(gamma))*(theta_sat-theta_0))...
        /(cos(gamma))*log(1+(inf_control_0(l-1)*cos(gamma)/...
        ((psi+y*cos(gamma))*(theta_sat-theta_0))));

        if abs(inf-inf_control_0(l-1)) < 0.01
```

```
            I_0 = inf_control_0(l-1);

            break

            else

            inf_control_0(l) = inf_control_0(l-1)+0.01;

            end

        end

        end
    end

    if (y*100) > tol_depth

        I(1) = I_0;     %Initial intfiltration set equal for all cells


    else

        I(1) = 0;

    end

end


%%%%%%%%%%%%%%%%%%%%%%%%%% Check for instabilities %%%%%%%%%%%%%%%%%%%%%%%

Cr = (abs(u)+sqrt(9.81*y))/(deltax/timestep);

if Cr > 1

disp('Courant number exceeded! Check input parameters, reduce timestep');

    break
end
```

```
%%%%%%%%%%%%%%%%%%%%% 2. Repeat for each time step %%%%%%%%%%%%%%%%%%%%%%%%



%%%%%%%%%%%%%%%%%%%%%%%%%%%%%%%%%%%%%%%%%%%%%%%%%%%%%%%%%%%%%%%%%%%%%%%%%%%

%                               Main loop

%%%%%%%%%%%%%%%%%%%%%%%%%%%%%%%%%%%%%%%%%%%%%%%%%%%%%%%%%%%%%%%%%%%%%%%%%%%




time = timein(1);

for j=1:numb_it

    % Boundary inflow conditions

    for k=1:n-1
        if (timein(k)>time)
            break;
        end
        beta = (timein(k+1)-time)/(timein(k+1)-timein(k));

        q = qinn(k)*beta+qinn(k+1)*(1-beta);

%%%%%%%%%%%%%%%%%%% Iteration loop rectangualar channel %%%%%%%%%%%%%%%%%%%

        if shape == 1,
```

```
        y_old = zeros(1,200);
        y_new = zeros(1,200);

        for i = 2:200                % Internal iteration for normal depth

            y_old(1) = 1;

            y_new(i-1) = q/(manning*B*((B)/((B/y_old(i-1))+2))^(2/3)*...
                sqrt(slope));

            y_old(i) = y_new(i-1);

                if (abs(y_old(i)-y_old(i-1))) < 0.0001

                    y = y_old(i);

                    if y < tol_depth    %Dry cell control

                        y = tol_depth;

                    end

                    break

                end

        end

        A = B*y;
        u = q/A;
        R = A/(2*y+B);


%%%%%%%%%%%%%%%%%% Iteration loop trapezoidal channel %%%%%%%%%%%%%%%%%%%


        elseif shape == 2

            control_iter = zeros(1,1000);
```

```
    y_iter = zeros(1,1000);

for i = 2:5000                  %Internal iteration normal depth

control = q/(manning*sqrt(slope));

y_iter(1) = 0;

control_iter(i) = (B*y_iter(i-1)+z*(y_iter(i-1))^2)*...
    ((B*y_iter(i-1)+z*(y_iter(i-1))^2)/(sqrt(B+z*y_iter(i-1)...
    *(1+z^2))))^(2/3);

        if (abs(control-control_iter(i))) < 0.001

            y = y_iter(i-1);

            if y < tol_depth    %Dry cell limitation

                y = tol_depth;

            end

            break

        end

        y_iter(i) = y_iter(i-1)+0.001;  %Threshold accuracy 1mm

end

B_top = B+2*z*y;
A = ((B+B_top)/(2))*y;
u = q/A;
R = A/(B+2*sqrt(y^2+(z*y)^2));

end

%%%%%%%%%%%%%%%%%%%%%%%%%%%%%%%%%%%%%%%%%%%%%%%%%%%%%%%%%%%%%%%%%%%%%%%%%%%%
```

```
        velocity(1,1) = u;      %Preparing vectors for St. Venants
        velocity(1,2) = u;
        depth(1,1) = y;
        depth(1,2) = y;
        R_hyd(1,1) = R;
        R_hyd(1,2) = R;

     velocity(sections,1) = velocity(sections-1,2);
        depth(sections,1) = depth(sections-1,2);
        R_hyd(sections,1) = R_hyd(sections-1,2);

        if shape == 2           %Parameters for trapezoidal discretization

            B_t(1,1) = B_top;
            B_t(1,2) = B_top;
            B_t(sections,1) = B_t(sections-1,2);

            area_trap(1,1) = A;
            area_trap(1,2) = A;
            area_trap(sections,1) = area_trap(sections-1,2);

        end

    end

%%%%%%%%%%%%%%%%% Water depth according to Eq. (5.10) %%%%%%%%%%%%%%%%%%%%

    for i=2:sections

        if shape == 1,



            depth(i,2) = depth(i,1)-timestep/(2.0*deltax)*(velocity(i,1)*...
            (depth(i+1,1)-depth(i-1,1))+depth(i,1)*...
            (velocity(i+1,1)-velocity(i-1,1)));
```

```
            R_hyd(i,2) = (B*depth(i,2))/(2*depth(i,2)+B);

            if depth(i,2) < tol_depth           %Dry cell control

                depth(i,2) = tol_depth;

            end

        end

        if shape == 2,

        depth(i,2) = depth(i,1)-((2*timestep)/(B+B_t(i,1)))*...
            (velocity(i,1))*(((B+B_t(i,1))/2)*((depth(i+1,1)+...
            depth(i-1,1))/(2*deltax))*((B+B_t(i,1))/(2))*depth(i,1)*...
            ((velocity(i+1,1)+velocity(i-1,1))/(2*deltax)));

        if depth(i,2) < tol_depth           %Dry cell control

            depth(i,2) = tol_depth;

        end

        B_t(i,2) = B+2*z*depth(i,2);
        area_trap(i,2) = ((B+B_t(i,2))/2)*depth(i,2);
        R_hyd(i,2) = area_trap(i,2)/...
            (B+2*sqrt((depth(i,2))^2+(z*depth(i,2))^2));

        end

    end

%%%%%%%% Compute the water velocity from full St.Venant Eq. (5.7) %%%%%%%%

    for i=2:sections

       if depth(i,2) < tol_depth

           velocity(i,2) = 0;
```

```
       else

dummy = -velocity(i,1)*timestep*0.5/deltax...
            *(velocity(i+1,1)-velocity(i-1,1));
dummy = dummy + -9.81*(timestep*0.5/deltax)*(depth(i+1,1)-...
            depth(i-1,1));
dummy = dummy + 9.81*slope*timestep;
dummy = dummy + - velocity(i,1)*velocity(i,1)*timestep*9.81...
            /(((R_hyd(i,1))^1.3333)*manning*manning);
velocity(i,2) = velocity(i,1) + dummy;

        end
    end

%%%%%%%%%%%% Correcting depth according to Eq. (6.8) %%%%%%%%%%%%%%%%%%%%

    for i=2:sections

       if depth(i,2) < tol_depth

           depth(i,2) = tol_depth;
           velocity(i,2) = 0;

        else

u = 0.5*(velocity(i,1)+velocity(i,2));
depth(i,2) = (0.5*(velocity(i-1,2)+velocity(i-1,1))*depth(i-1,2)+...
            depth(i,1)*(deltax/timestep-0.5*u))/...
            (deltax/timestep+0.5*u);

            if shape == 1

            R_hyd(i,2) = (B*depth(i,2))/(2*depth(i,2)+B);

            elseif shape == 2

            B_t(i,2) = B+2*z*depth(i,2);
            area_trap(i,2) = ((B+B_t(i,2))/2)*depth(i,2);
```

```
            R_hyd(i,2) = area_trap(i,2)/...
                (B+2*sqrt((depth(i,2))^2+(z*depth(i,2))^2));

            end

        end

        if shape == 1

            A(i,2) = depth(i,2)*B;

        end

        if shape == 2

            B_t(i,2) = B+2*depth(i,2)*z;
            A(i,2) = ((B+B_t(i,2))/2)*depth(i,2);

        end

    end

%%%%%%%%%%%%%%%% Infiltration step solving Eq. (5.12) %%%%%%%%%%%%%%%%%%%%

    if infiltration_step == 1               %Calculates infiltration in cm

        inf_length = inf_length+max(velocity(1:sections,2))*timestep;

        if inf_length > length

            inf_length = length;

        end

        depth_avg = mean(depth(1:sections,2));
        %Mean channel flow depth in current timestep

        if j == 1
```

```
    I(j) = I_0;

else

    if I(j-1) < z_tot
    %Infiltration only if wetting front has not reached matrix
    %depth.

    if solver == 1  %Symbolic solver

    syms I_solver

    old = digits;

    digits(10);     %Solver accuracy

    I_temp = vpasolve(K_sat*(time/(60*60))*cos(gamma)...
        +((psi+depth_avg*100*cos(gamma))*(theta_sat-theta_0))...
        /(cos(gamma))*log(1+(I_solver*cos(gamma)/...
        ((psi+depth_avg*cos(gamma))*(theta_sat-theta_0))))==...
        I_solver, I_solver, K_sat*(time/(60*60))*cos(gamma));

    double(I_temp);

    digits(old);

    elseif solver == 2  %Numerical solver

    for l = 2:3000

        inf_control(1) = K_sat*(time/(60*60))*cos(gamma);

        inf = K_sat*(time/(60*60))*cos(gamma)...
            +((psi+depth_avg*100*cos(gamma))*(theta_sat-theta_0))...
            /(cos(gamma))*log(1+(inf_control(l-1)*cos(gamma)/...
            ((psi+depth_avg*cos(gamma))*(theta_sat-theta_0))));

        if abs(inf-inf_control(l-1)) < 0.001
```

```
                I_temp = inf_control(l-1);
                %disp(l);   counter to track number og necessary
                %iterations

                break

            else

                inf_control(l) = inf_control(l-1)+0.01;

            end

        end

        end

            I(j) = I_temp;

            I_diff(j) = I(j)-I(j-1);
            %Change in infiltrated amount [cm] per section per timestep

        else

            I(j) = z_tot;

            I_diff(j) = 0;

        end

    end

        if shape == 1

            I_vol(j) = (I(j)/100)*inf_length*B;
            %Cummulative infiltrated volume per section per timestep in
            %m^3

        end
```

```
            if shape == 2

                B_t_avg = mean(B_t(1:sections,1));
                I_vol(j) = (I(j)/100)*inf_length*B_t_avg;
                %Cummulative infiltrated volume per section per timestep in
                %m^3

            end


%%%%%%%%%%%%%%%%%%Reduce depth as a result of infiltration%%%%%%%%%%%%%%%


            for i = 2:sections

                if I_diff(j) < 0.1

                %Tolerance demand in order to disregard false oscillations
                %in Green Ampt

                depth(i,2) = depth(i,2)-abs(I_diff(j))/100;

                if I_diff(j)/100 > depth(i,2)

                    depth(i,2) = tol_depth;

                elseif depth(i,2) < tol_depth

                    depth(i,2) = tol_depth;

                end

                end

            end

    end
```

```
%%%%%%%%%%%%%%%%%%%%%%%%%%%%%%%%%%%%%%%%%%%%%%%%%%%%%%%%%%%%%%%%%%%%%%%%%%%%%%%%

    % Updating variables

    for i = 2:sections

        if shape == 1

            area_rect(i,1) = area_rect(i,2);

        elseif shape == 2

            B_t(i,1) = B_t(i,2);
            area_trap(i,1) = area_trap(i,2);

        end

        velocity(i,1) = velocity(i,2);
        depth(i,1) = depth(i,2);
        R_hyd(i,1) = R_hyd(i,2);

    end

%%%%%%%%%%%%%%%%%%%%%%%%%% Check for instabilities %%%%%%%%%%%%%%%%%%%%%%%%%%

        Cr = (abs(u)+sqrt(9.81*y))/(deltax/timestep);

            if Cr > 1

                disp('Break on iteration number: ');
                disp(j);
                disp('Courant number exceeded! Reduce timestep.');

                break

            end

    time = time + timestep;         %Increasing timestep for entire loop
```

```
    %disp(j);                          %Counter to track progress of main loop

%%%%%%%%%%%%%%%%%%%%%%%%%%%% Printing to file %%%%%%%%%%%%%%%%%%%%%%%%%%%%

    tab_q(:,1)=time;
    tab_q(:,2)=velocity(2,2)*A(2,2);
    tab_q(:,3)=velocity((length/deltax)-1,2)*A((length/deltax)-1,2);
    dlmwrite('outflow.txt', tab_q, 'delimiter', ' ',...
        '-append', 'precision', '%.6f')

    tab_y(:,1) = time;
    tab_y(:,2) = depth(2,2);
    tab_y(:,3) = depth((length/deltax)-1,2);
    dlmwrite('depth.txt', tab_y, 'delimiter', ' ',...
        '-append', 'precision', '%.6f')

    tab_u(:,1) = time;
    tab_u(:,2) = velocity(2,2);
    tab_u(:,3) = velocity((length/deltax)-1,2);
    dlmwrite('velocity.txt', tab_u, 'delimiter',...
        ' ', '-append', 'precision', '%.6f')

    if infiltration_step == 1

    tab_inf(:,1) = time;
    tab_inf(:,2) = I_vol(j);
    tab_inf(:,3) = I(j);
    dlmwrite('infiltration.txt', tab_inf,...
        'delimiter', ' ', '-append', 'precision', '%.6f')

    end


end

%%%%%%%%%%%%%%%%%%%%%%%% Plotting discharge %%%%%%%%%%%%%%%%%%%%%%%%%%%%%%%
```

```
temp_q = load('outflow.txt');
a_q = temp_q(:,1);
b_q = temp_q(:,2);
c_q = temp_q(:,3);

if infiltration_step == 1

    temp_inf = load('infiltration.txt');
    a_inf = temp_inf(:,1);
    b_inf = temp_inf(:,2);

end

h_q = figure('Visible','off');

if infiltration_step == 1

[haxes,hline1,hline2] = plotyy(a_q, [b_q c_q], a_q, b_inf,'plot');
set(haxes(1), 'YLim', [0 max(b_q)])
set(haxes(1), 'YTick', 0:0.1:max(b_q))
set(haxes(2), 'YLim', [min(b_inf) max(b_inf)])
set(haxes(2), 'YTick', 0:5:max(b_inf))
set(haxes(1), 'Xlim', [0 max(a_q)])
set(haxes(2), 'XLim', [0 max(a_q)])
title('Discharge - Infiltration')
xlabel(haxes(2), 'Time[s]')
ylabel(haxes(1), 'm^3/s')
ylabel(haxes(2), 'm^3', 'Color', 'k')
set(hline1, 'LineStyle', '-', {'Color'}, {[0.6 0 0.5];[0.7 0.6 0]},...
    'LineWidth', 1.5)
set(hline2, 'LineStyle', '-.', 'Color', [0 0.5 0.6], 'Linewidth', 1.5)
set(haxes, {'ycolor'},{'k';'k'})
legend('Inflow','Outflow','Cumulative infiltration')
legend('Location', 'East')
figureHandle = gcf;
set(findall(figureHandle, 'type', 'text'), 'fontSize', 16)
set(gca, 'FontName', 'Helvetica')
set(gca,...
```

```
    'Box', 'off', 'Tickdir', 'out', 'TickLength', [.02 .02],...
    'XminorTick', 'on', 'YMinorTick', 'on', 'Ygrid', 'on')
set(haxes(2), 'XTick', [], 'XTicklab', [])


print(h_q,'-dpng', '-r125', [['Discharge - Infiltration, ','Timestep = ',...
    num2str(timestep), ', Cross Section = ', num2str(shape), ', S_0 = ',...
    num2str(slope), ', M = ', num2str(manning)], ', Soiltype = ',...
    num2str(soiltype), ', Initial Saturation = ', num2str(theta_0),...
    '.png'])


else
p = plot(a_q, b_q, '-', a_q, c_q, '-');
axis([0 max(a_q) 0 max(b_q)])
title('Discharge')
xlabel('Time [s]')
ylabel('Discharge [m3/s]')
set(p, 'Linestyle', '-', {'Color'}, {[0.6 0 0.5];[0.7 0.6 0]},...
    'LineWidth', 1.5)
legend('Inflow', 'Outflow')
legend('Location', 'East')
set(gca, 'FontName', 'Helvetica')
figureHandle = gcf;
set(findall(figureHandle, 'type', 'text'), 'fontSize', 16)
set(gca,...
    'Box', 'off', 'Tickdir', 'out', 'TickLength', [.02 .02],...
    'XminorTick', 'on', 'YMinorTick', 'on', 'Ygrid', 'on')

print(h_q,'-dpng', '-r125', [['Discharge, ','Timestep = ',...
    num2str(timestep), ', Cross Section = ', num2str(shape), ', S_0 = ',...
    num2str(slope), ', M = ', num2str(manning)],'.png'])

end
close(h_q)

%%%%%%%%%%%%%%%%%%%%%%%%%% Plotting depth %%%%%%%%%%%%%%%%%%%%%%%%%%%%%%

temp_y = load('depth.txt');
```

```
a_y = temp_y(:,1);
b_y = temp_y(:,2);
c_y = temp_y(:,3);
h_y = figure('Visible','off');

py = plot(a_y,[b_y c_y]);
axis([0 max(a_y) 0 max(b_y)])
title('Depth')
xlabel('Time [s]')
ylabel('Depth [m]')
set(py, 'Linestyle', '-', {'Color'}, {[0.6 0 0.9];[0.2 0.6 0.5]},...
    'LineWidth', 1.5)
legend('Inflow', 'Outflow')
legend('Location', 'East')
figureHandle = gcf;
set(gca, 'FontName', 'Helvetica')
set(findall(figureHandle, 'type', 'text'), 'fontSize', 16)
set(gca,...
    'Box', 'off', 'Tickdir', 'out', 'TickLength', [.02 .02],...
    'XminorTick', 'on', 'YMinorTick', 'on', 'Ygrid', 'on')


if infiltration_step == 1

print(h_y,'-dpng', '-r125', [['Depth, ','Timestep = ',...
    num2str(timestep), ', Cross Section = ', num2str(shape), ', S_0 = ',...
    num2str(slope), ', M = ', num2str(manning)], ', Soiltype = ',...
    num2str(soiltype), ', Initial Saturation = ', num2str(theta_0),...
    '.png'])

else

print(h_y,'-dpng', '-r125', [['Depth, ','Timestep = ',...
    num2str(timestep), ', Cross Section = ', num2str(shape), ', S_0 = ',...
    num2str(slope), ', M = ', num2str(manning)],'.png'])

end

close(h_y)
```

```
%%%%%%%%%%%%%%%%%%%%%%%%%%%%% Plotting velocity %%%%%%%%%%%%%%%%%%%%%%%%%%%%%

temp_u = load('velocity.txt');
a_u = temp_u(:,1);
b_u = temp_u(:,2);
c_u = temp_u(:,3);

h_u = figure('Visible','off');

pu = plot(a_u,[b_u c_u]);
axis([0 max(a_u) 0 max(b_u)])
title('Velocity')
xlabel('Time [s]')
ylabel('Velocity [m/s]')
set(pu, 'Linestyle', '-', {'Color'}, {[0.3 0.7 0.2];[1 0.5 0.1]},...
    'LineWidth', 1.5)
legend('Inflow', 'Outflow')
legend('Location', 'East')
set(gca, 'FontName', 'Helvetica')
figureHandle = gcf;
set(findall(figureHandle, 'type', 'text'), 'fontSize', 16)
set(gca,...
    'Box', 'off', 'Tickdir', 'out', 'TickLength', [.02 .02],...
    'XminorTick', 'on', 'YMinorTick', 'on', 'Ygrid', 'on')

if infiltration_step == 1

print(h_u,'-dpng', '-r125', [['Velocity, ','Timestep = ',...
    num2str(timestep), ', Cross Section = ', num2str(shape), ', S_0 = ',...
    num2str(slope), ', M = ', num2str(manning)], ', Soiltype = ',...
    num2str(soiltype), ', Initial Saturation = ', num2str(theta_0),...
    '.png'])

else

print(h_u,'-dpng', '-r125', [['Velocity, ','Timestep = ',...
    num2str(timestep), ', Cross Section = ', num2str(shape), ', S_0 = ',...
    num2str(slope), ', M = ', num2str(manning)],'.png'])
```

```
end
close(h_u)

%%%%%%%%%%%%%%%%%%%%%% Plotting infiltration %%%%%%%%%%%%%%%%%%%%%%%%%%%%%%

if infiltration_step == 1

temp_inf = load('infiltration.txt');
a_inf = temp_inf(:,1);
b_inf = temp_inf(:,2);
c_inf = temp_inf(:,3);

h_inf = figure('Visible','off');

[haxesi,hline1i,hline2i] = plotyy(a_inf, b_inf, a_inf, c_inf,'plot');
set(haxesi(1), 'YLim', [min(b_inf) max(b_inf)])
set(haxesi(1), 'YTick', 0:5:max(b_inf))
set(haxesi(2), 'YLim', [min(c_inf) max(c_inf)])
set(haxesi(2), 'YTick', 0:5:max(c_inf))
set(haxesi(1), 'Xlim', [0 max(a_inf)])
set(haxesi(2), 'Xlim', [0 max(a_inf)])
title({'Cumulative volumetric infiltration';...
    'Cumulative infiltration depth'})
xlabel(haxesi(2), 'Time[s]')
ylabel(haxesi(1), 'm^3')
ylabel(haxesi(2), 'cm', 'Color', 'k')
set(hline1i, 'LineStyle', '-.', 'Color', [0.6 0 0.5], 'LineWidth', 2)
set(hline2i, 'LineStyle', ':', 'Color', [0 0.5 0.6], 'Linewidth', 2)
set(haxesi, {'ycolor'},{'k';'k'})
legend('Cumulative volume', 'Cumulative depth')
legend('Location', 'East')
set(gca, 'FontName', 'Helvetica')
figureHandle = gcf;
set(findall(figureHandle, 'type', 'text'), 'fontSize', 16)
set(gca,...
    'Box', 'off', 'Tickdir', 'out', 'TickLength', [.02 .02],...
    'XminorTick', 'on', 'YMinorTick', 'on', 'Ygrid', 'on')
set(haxesi(2), 'XTick', [], 'XTicklab', [])
```

```
print(h_q,'-dpng', '-r125', [['Infiltration, ','Timestep = ',...
    num2str(timestep), ', Cross Section = ', num2str(shape), ', S_0 = ',...
    num2str(slope), ', M = ', num2str(manning)], ', Soiltype = ',...
    num2str(soiltype), ', Initial Saturation = ', num2str(theta_0),...
    '.png'])

close(h_inf)

end


disp('Finished!')
```